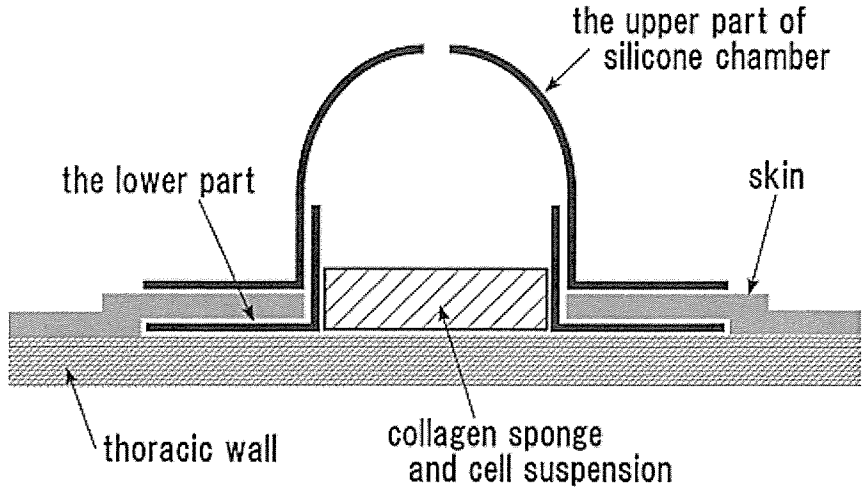

FIG 1. Scheme of the hair reconstitution assay, using a collagen sponge as the scaffold.

Evaluation of grafted sites

The grafts were observed daily for the first 10 days after grafting, and after that every other day for up to 3 weeks. Before the histological examination of the grafted sites, all hairs grown up from each grafted site were cut and spread on paper for counting. The graft site area was then measured to calculate the density of hair growth ($n = 3$ for each group). For histological examination, the grafted sites were excised, fixed in 10% formaldehyde (Wako, Osaka, Japan) at room temperature for 1–2 h, and processed for paraffin sectioning. Histological sections (8 μm thick) were stained with hematoxylin and eosin. Moreover, the number of epidermal cysts formed in the selected area of each grafted site was counted ($n = 5$ for each group). The selected area was defined as an 80% area in the center of the middle section of a fixed grafted site.

RESULTS

Appearance and intrastructure of collagen sponges

Figure 2 shows SEM photographs of cross-sections of collagen sponge with or without PGA fiber. Irrespective of the incorporated fiber, collagen sponge possessed an interconnected porous structure with an almost homogeneous pore size. Although PGA fibers were exposed in the pores of PGA-incorporated sponges, the internal structure was similar to that of sponge without PGA fibers.

Macroscopic analysis of grafted sites

To evaluate the effect of the conventional collagen PGA(–) sponge and PGA(+) sponge on the formation of

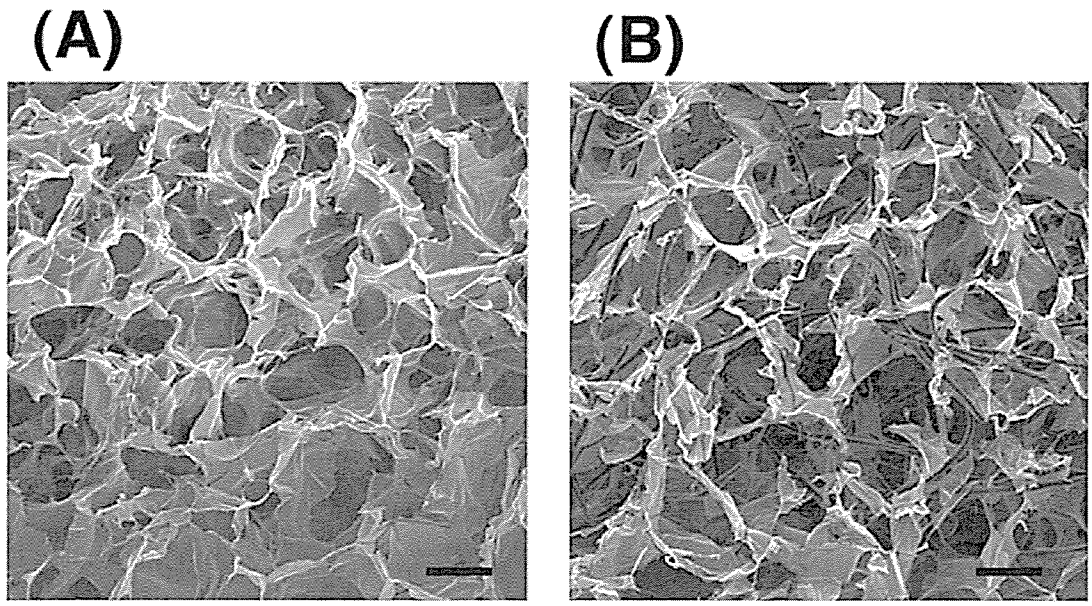

FIG 2. Cross-sectional SEM photographs of collagen sponge (**A**) and collagen sponge incorporating PGA fiber (**B**). Scale bars: 200 μm.

hair in the reconstitution assay, we observed the appearance of the grafted sites for up to 3 weeks, when hair reconstitution is normally completed. On the grafted areas of the PGA(–) sponge, the hair follicles were observed for 1 week. However, the hair growth was poor and sparse, as shown in Fig. 3A and B. The size of the fixed grafted sites extended beyond the size of original sponge (Fig. 3A). Moreover, ectopic hair growth was seen macroscopically under the skin around the graft site (Fig. 3C).

When the grafts were made on a PGA(+) sponge, hair formation was induced 10–12 days after grafting, slightly later than on the PGA(–) sponge. However, the hairs on the PGA(+) sponge were very thick and grew properly, compared with those on the PGA(–) sponge (Fig. 3D and E). Quantitative analysis of the hair density on each graft demonstrated that mean hair density was 531 ± 179 and 2808 ± 1237 hairs/cm^2 on PGA(–) and PGA(+) sponge, respectively (Fig. 4A). The size and shape of the grafted sites on the PGA(+) sponge stayed unchanged in comparison with the original sponge size. Little ectopic hair growth was noted (Fig. 3F). Moreover, hair and hair follicles grafted on the athymic mice were maintained for 6 months at least. Collectively, these data suggest that the PGA(+) sponge is more advantageous for hair growth.

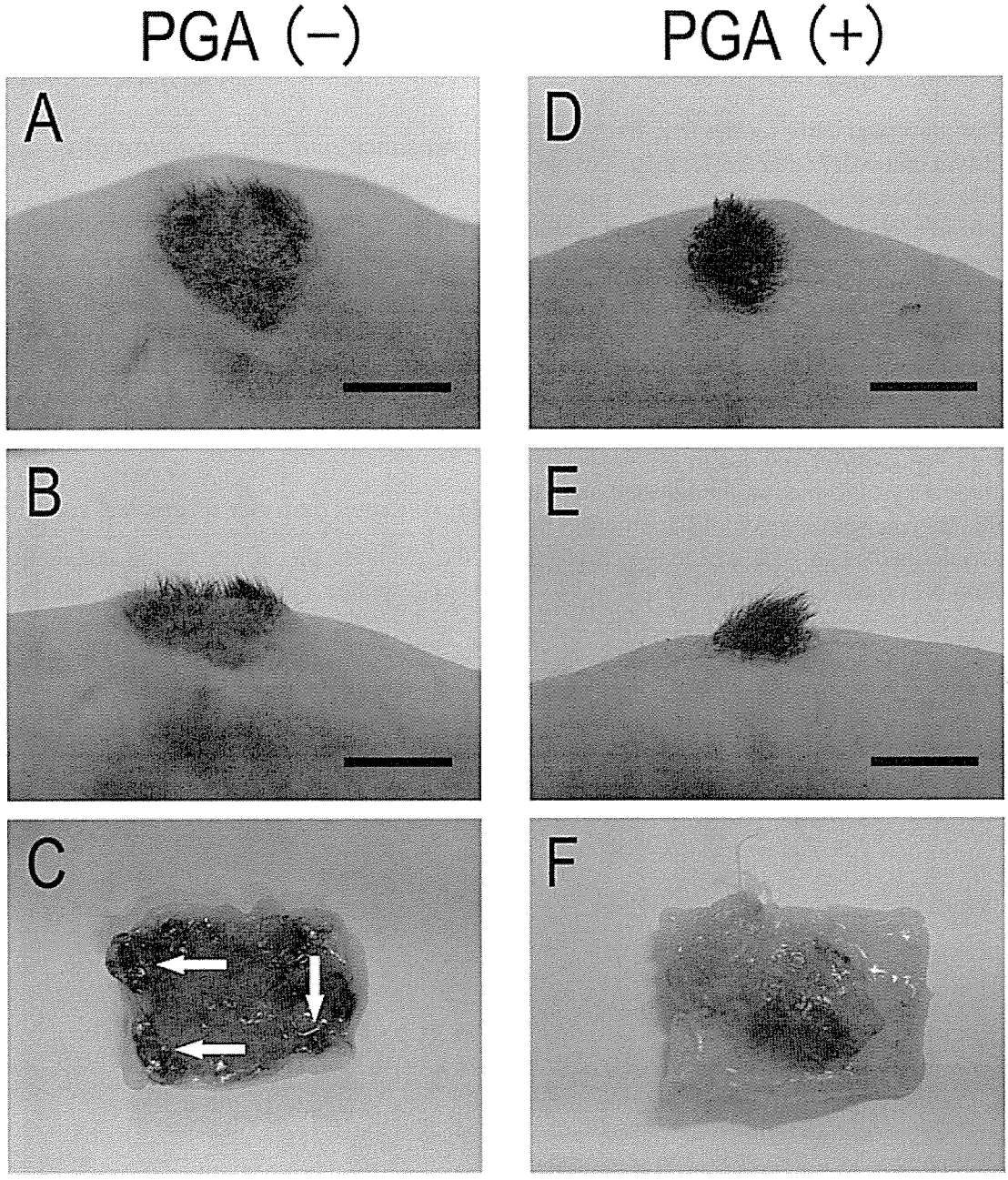

FIG 3. Macroscopic appearance of the grafted sites on PGA(–) sponge (**A–C**) and PGA(+) sponge (**D–F**). (**A** and **D**) Overview; (**B** and **E**) lateral view; (**C** and **F**) back side of the grafted site. Much ectopic hair formation (arrows) was seen under the skin around the site (**C**). Scale bars: 1 cm.

Histological examination

The grafts were then examined histologically. Although the basic structure of the skin, that is, the epidermis and dermis, was reconstituted, every grafted site on the PGA(–) sponges contained epidermal cysts within the dermis and ectopic hair formation under the skin (Fig. 4B and Fig. 5A and B). Even when the hair sprouted out of the skin, the array was slightly disheveled. In some cases, many epidermal cysts were formed (9.6 ± 3.2 cysts/section), inasmuch that normal hair formation was completely disturbed (Fig. 5C and D).

In the case of the PGA(+) sponge, few epidermis cysts were observed (1.4 ± 1.1 cysts/section), and ectopic hair formation was far less than on PGA(–) sponge (Fig. 4B and Fig. 5E and G). Furthermore, on the PGA(+) sponge, the hair array was arranged regularly, sloping from head to tail. Sebaceous glands were normally generated.

The PGA(+) collagen sponge as a scaffolding did not seem to interfere with normal hair formation and outgrowth in the hair reconstitution assay.

DISCUSSION

In the current study, we attempted to make the hair reconstitution assay more convenient and precise, by using a collagen sponge as a scaffold. Because collagen, the main component of the extracellular matrix, has superior cell affinity than other, synthetic molecules, it has been commonly used as a scaffold in three-dimensional skin reconstitution cultures, in which the construction of a structure suggestive of normal skin is generated *in vitro*.[16–19] In a three-dimensional skin culture using collagen sponges, a multilayered skin structure can be reconstituted. However, current three-dimensional reconstituted skin has no skin appendages, including hair follicles and sweat/sebaceous glands. Thus, the influence of collagen sponges on the formation of skin appendages has not been investigated. Using a collagen sponge as a scaffold in this hair reconstitution assay, the method became more convenient and we could obtain highly reproducible results, that is, the rate of fixation and the appearance of every grafted site, compared with established methods, and we could perform quantitative evaluations such as hair density analysis. Such results suggest that the sponge could retain the grafted cells within itself and prevent the cell suspension from tilting and leaking out of the chamber. However, our study demonstrated that the conventional collagen sponge disturbed normal hair reconstitution. Therefore, we prepared a novel collagen sponge reinforced by PGA fiber, and this study suggests that normal hair growth can be seen at the grafted sites of the PGA(+) sponge, as compared with the conventional PGA(–) sponges.

Our results showed that epidermal cysts and ectopic hairs frequently formed on the conventional PGA(–) collagen sponge. One possible reason is that the volume of the PGA(–) sponge decreased as a result of humidity after the seeding of cell suspension, because collagen was weaker. Thus, because the pore structure size of the sponge shrank, the deflated collagen sponge might inhibit the movement of the transferred cells, with epidermal cysts consequently forming in the grafted sites. Moreover, the shrinkage of PGA(–) sponges might also result in the leakage of cell suspension that could not be retained within the collagen sponge. Therefore, it might cause enlargement of the grafted sites and ectopic hair formation. Thus, with use of the conventional sponge alone, the proper reconstitution of hair follicles cannot be fully achieved.

The synthetic polymers PGA and poly-L-lactic acid (PLLA) have been commonly used in clinical fields. The time over which PGA biodegrades (approximately 1

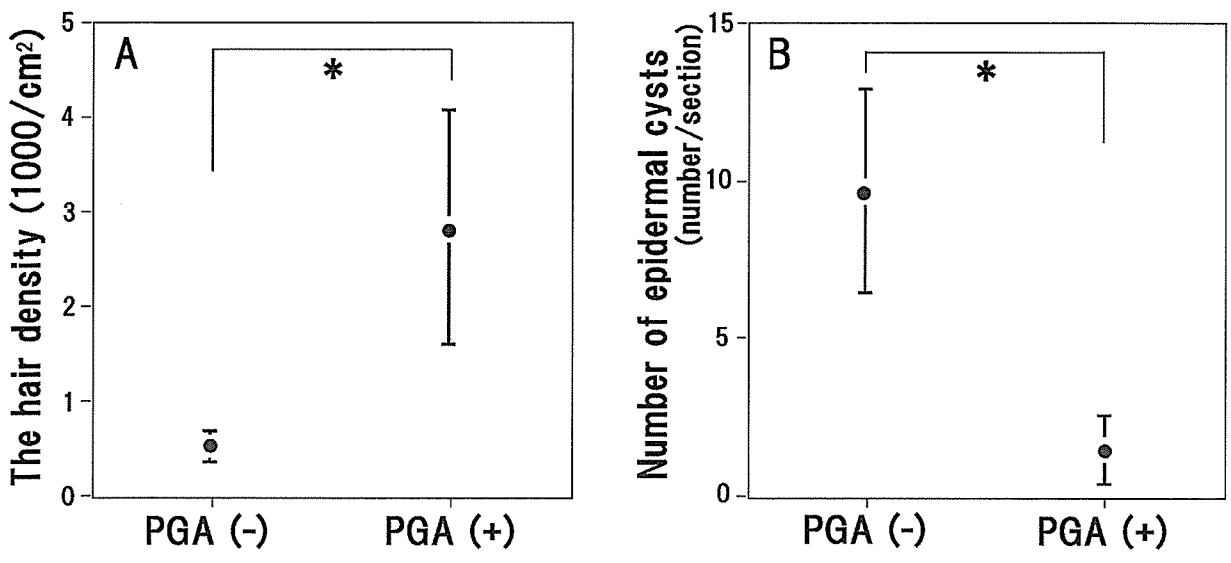

FIG 4. Hair density (**A**) and number of epidermal cysts (**B**) on the grafted site. $*p < 0.05$.

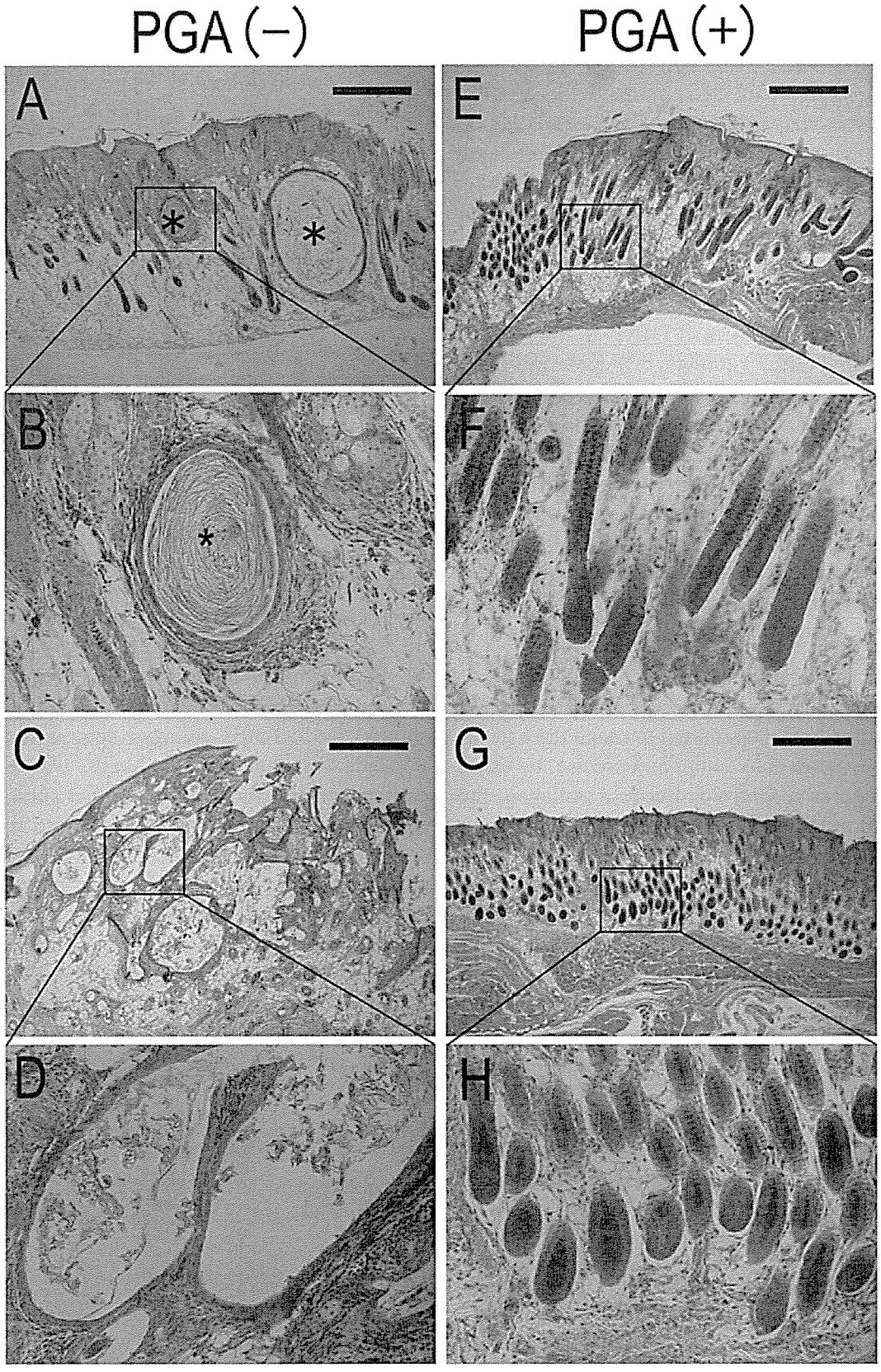

FIG 5. Microscopic appearance of the grafted sites on PGA(–) sponge (**A–D**) and PGA(+) sponge (**E–H**). On PGA(–) sponge, epidermal cyst formation (**A** and **B,** asterisk) and disturbed hair formation (**C** and **D**) were frequently observed. (**E–H**) Hair array was arranged regularly on PGA(+) sponge. Scale bars: 500 μm. Original magnification: (**A, C, E,** and **G**) ×40; (**B, D, F,** and **H**) ×200. H&E staining.

month) is much shorter than that of PLLA, (approximately 2 years). Moreover, the biocompatibility of PGA is better than that of PLLA, but neither is as good as collagen.[14] We then created a novel scaffold, which has the advantageous properties of both collagen and synthetic polymer, using PGA fiber. Because the incorporation of PGA fibers mechanically reinforces the collagen sponge, the PGA(+) sponge had less shrinkage, thereby maintain-

ing the size of the pore structure in the sponge. Therefore, because the PGA(+) sponge can accept and keep a sufficient volume of the cell mixture, the grafted cells can be retained within the sponge. Perhaps because of this, little ectopic hair formation was observed in the grafted sites of the PGA(+) sponge. Furthermore, the movement of the transferred cells did not seem to be inhibited in the PGA(+) sponge, and as a result this may have suppressed the formation of epidermal cysts. Thus, it is likely that not only the cellular requirements but also the cell positions and movements are important for proper restructuring of hair follicles, inferring from the process of hair morphogenesis that the epithelium grows downward into the dermis as a plug that joins at its proximal end a mesenchymal condensation, referred to as the dermal papilla.[1,2]

Moreover, because the incorporation of PGA fibers confers to the collagen sponge the ability to resist mechanical deformation, the PGA(+) sponge has the ability to be transformed into various shapes, raising the possibility that it could be embedded as a scaffold even on an irregular graft bed. Future advances in the cell biological study of hair formation may, using the PGA(+) collagen sponge, allow for three-dimensional skin reconstitution cultures with skin appendages and subsequent cell transplantation therapy into patients.

ACKNOWLEDGMENTS

The authors thank Dr. Steven D. Emmet for advice on preparing the manuscript in English. This work was supported by a health science research grant from the Japanese Ministry of Health, Labor, and Welfare.

REFERENCES

1. Stenn, K.S., and Paus, R. Controls of hair follicle cycling. Physiol. Rev. **81,** 449, 2001.
2. Millar, S.E. Molecular mechanisms regulating hair follicle development. J. Invest. Dermatol. **118,** 216, 2002.
3. Alonso, L., and Fuch, E. Stem cell in the skin: Waste not, Wnt not. Genes Dev. **17,** 1189, 2003.
4. Worst, P.K.M., Mackenzie, I.C., and Fusenig, N.E. Reformation of organized epidermal structure by transplantation of suspensions and cultures of epidermal and dermal cells. Cell Tissue Res. **225,** 65, 1982.
5. Kamimura, J., Lee, D., Baden, H.P., Brissette, J., and Dotto, G.P. Primary mouse keratinocyte cultures contain hair follicle progenitor cells with multiple differentiation potential. J. Invest. Dermatol. **109,** 534, 1997.
6. Lichti, U., Weinberg, W.C., Goodman, L., Ledbetter, S., Dooley, T., Morgan, D., and Yuspa, S.H. In vivo regulation of murine hair growth: Insights from grafting defined cell populations onto nude mice. J. Invest. Dermatol. **101,** 124s, 1993.
7. Weinberg, W.C., Goodman, L.V., George, C., Morgan, D.L., Ledbetter, S., Yuspa, S.H., and Lichti, U. Reconstitution of hair follicle development in vitro: Determination of follicle formation, hair growth, and hair quality by dermal cells. J. Invest. Dermatol. **100,** 229, 1993.
8. Kishimoto, J., Ehama, R., Wu, L., Jiang, S., Jiang, N., and Burgeson, R.E. Selective activation of the versican promoter by epithelial–mesenchymal interactions during hair follicle development. Proc. Natl. Acad. Sci. U.S.A. **96,** 7336, 1999.
9. Cotsarelis, G., Sun, T., and Lavker, R.M. Label-retaining cells reside in the bulge area of pilosebaceous unit: Implications for follicular stem cells, hair cycle, and skin carcinogenesis. Cell **61,** 1329, 1990.
10. Kobayashi, K., Rochat, A., and Barradon, Y. Segregation of keratinocyte colony-forming cells in the bulge of the rat vibrissa. Proc. Natl. Acad. Sci. U.S.A. **90,** 7391, 1993.
11. Rochat, A., Kobayashi, K., and Barrandon, Y. Location of stem cells of human hair follicles by clonal analysis. Cell **76,** 1063, 1994.
12. Oshima, H., Rochat, A., Kedzia, C., Kobayashi, K., and Barrandon, Y. Morphogenesis and renewal of hair follicles from adult multipotent stem cells. Cell **104,** 233, 2001.
13. Yuspa, S.H., Morgan, D.L., Walker, R.J., and Bates, R.R. The growth of fetal mouse skin in cell culture and transplantation to F_1 mice. J. Invest. Dermatol. **55,** 379, 1970.
14. Ueda, H., and Tabata, Y. Polyhydroxyalkanonate derivatives in current clinical applications and trials. Adv. Drug Deliv. Rev. **55,** 501, 2003.
15. Hiraoka, Y., Agr, M., Kimura, Y., Eng, M., Ueda, H., and Tabata, Y. Fabrication and biocompatibility of collagen sponge reinforced with poly(glycolic acid) fiber. Tissue Eng. **9,** 1101, 2003.
16. Yannas, I.V., and Burke, J.F. Design of an artificial skin. I. Basic design principles. J. Biomed. Mater. Res. **14,** 65, 1980.
17. Bell, E., Ehrlich, H.P., Buttle, D.J., and Nakatsuji, T. Living tissue formed in vitro and accepted as skin-equivalent tissue of full thickness. Science **211,** 1052, 1981.
18. Hansbrough, J.F., Boyce, S.T., Cooper, M.L., and Foreman, T.J. Burn wound closure with cultured autologous keratinocytes and fibroblasts attached to a collagen–glycosaminoglycan substrate. JAMA **262,** 2125, 1989.
19. Maruguchi, T., Maruguchi, Y., Suzuki, S., Matsuda, K., Toda, K., and Isshiki, N. A new skin equivalent: Keratinocytes proliferated and differentiated on collagen sponge containing fibroblasts. Plast. Reconst. Surg. **93,** 537, 1994.

Address reprint requests to:
Hitoshi Okochi, M.D., Ph.D.
Department of Tissue Regeneration
Research Institute, International Medical Center of Japan
1-21-1 Toyama, Shinjuku-ku, Tokyo 162-8655, Japan

E-mail: hokochi@ri.imcj.go.jp

DNA Cleavage

A Synthetic Block Copolymer Regulates S1 Nuclease Fragmentation of Supercoiled Plasmid DNA**

*Kensuke Osada, Yuichi Yamasaki, Satoshi Katayose, and Kazunori Kataoka**

The materials chemistry and physics of block copolymer supramolecular assembly continue to receive considerable attention in the construction of higher-ordered architectures with unique morphologies and functions.[1–10] Of particular

[*] Dr. K. Osada, Dr. Y. Yamasaki, Prof. Dr. K. Kataoka
Department of Materials Science and Engineering
Graduate School of Engineering, The University of Tokyo
Hongo 7-3-1, Bunkyo, Tokyo 113-8655 (Japan)
Fax: (+81) 3-5841-7139
E-mail: kataoka@bmw.t.u-tokyo.ac.jp
Dr. S. Katayose[+]
Department of Materials Science and Engineering
Tokyo University of Science
Yamazaki 2641, Noda, Chiba 278 (Japan)
[+] Present address:
Tsukuba Research Laboratories
JSR Corporation
25 Miyukigaoka, Tsukuba, Ibaraki 305-0841 (Japan)

[**] This work was supported by The Special Coordination Funds for Promoting Science and Technology, a Grant-in-Aid for Scientific Research on Priority Area A (Molecular Synchronization for Design of New Materials System) from the Ministry of Education, Culture, Sports, Science, and Technology (MEXT), and the Core Research Program for Evolutional Science and Technology (CREST) from the Japan Science and Technology Corporation (JST). The authors thank D. W. Grainger for critical reading of the manuscript.

Supporting Information for this article is available on the WWW under http://www.angewandte.org or from the author.

  DOI: 10.1002/anie.200500201

interest is the exploitation of the spatial order intrinsic to block copolymers for the amplification or modulation of molecular recognition processes by using integrated multisite interactions as well as a distinct spatial matching. Herein we report an unprecedented finding that DNA supramolecular assembly with the synthetic block copolymer poly(ethylene glycol)-*b*-poly(L-lysine) (PEG-PLL)[6,11–14] modulates supercoiled plasmid DNA into a particular structure. The incorporated DNA within the assembly is cleaved into seven distinct regular fragments by S1 nuclease, an enzyme known to cleave single-stranded DNA. The seven characteristic DNA fragments were of well-defined molecular sizes; in each case these were 10/12, 9/12, 8/12, 6/12, 4/12, 3/12, and 2/12 of the original plasmid length (Figure 1). It is notable that the cleaved sites

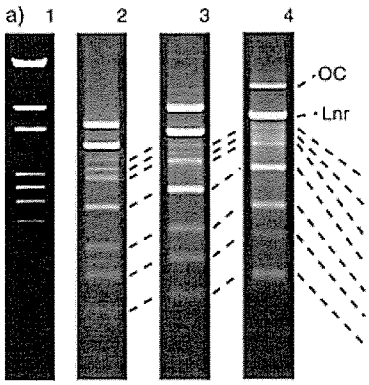

b)

Fragments

Length of the fragment [bp] / Size ratio to the native DNA [%]

no	pBR322 4363 bp	pGL3-Luc 5256 bp	ColE1 6646 bp	ratios in fraction
1	3690 / 84.6	4560 / 84.6	5630 / 84.8	10/12
2	3260 / 75.3	4100 / 76.1	5000 / 75.2	9/12
3	2940 / 67.4	3680 / 68.2	4490 / 67.6	8/12
4	2180 / 50.0	2740 / 50.8	3360 / 50.6	6/12
5	1460 / 33.5	1830 / 34.0	2240 / 33.7	4/12
6	1050 / 24.1	1340 / 24.9	1650 / 24.9	3/12
7	750 / 17.1	910 / 16.8	1090 / 16.4	2/12

Figure 1. Regulated fragmentation of plasmid DNAs complexed with PEG-PLL by the S1 nuclease: a) Gel electrophoresis results. Lane 1: marker DNA; lane 2: pBR322 (4363 bp); lane 3: pGL3-Luc (5256 bp); lane 4: ColE1 (6646 bp). OC = relaxed open circular DNA, Lnr = linearized DNA. b) Length of the obtained fragments and size ratio of them to the native DNA. The size ratio of each fragment from three plasmid DNAs is represented as a fraction in the right-hand column.

are located just outside of protein-coding regions, a fact which simultaneously indicates that the S1 nuclease cuts out genes from DNA.

The block copolymer used in this study comprises a cationic PLL segment, which is the plasmid-binding portion, and a nonionic PEG segment, which forms a hydrophilic and hydrated palisade surrounding the ion-paired complex between PLL and plasmid DNA (see the Supporting Information). This allows to obtain a water-soluble nanoscale assembly (100-nm size) without precipitation. The size-specific plasmid DNA cleavage by S1 nuclease was observed at an acidic pH value of 4.9 for the complex, particularly in a unit molar ratio (amino group/phosphate) of 1.0. As seen in lane 2 of Figure 1a, pBR322 DNA is cut into seven distinct fragments (as listed in Figure 1b). This regular fragmentation was not specific only for pBR322 but seems common for other plasmids. Surprisingly, the other plasmids, pGL3-Luc and ColE1, when complexed with PEG-PLL, were also cut into seven fragments of the same fractions when measured against each original plasmid (Figure 1a, lanes 3 and 4, and Figure 1b). The consistency of the fragmentation results clearly indicates the systematic cleavage of plasmid DNA at well-defined intervals. It should be noted that this regular cleavage of plasmid DNA complexed with PEG-PLL is only observed for the supercoiled DNA form. Relaxed open circular DNA, prepared by treatment with topoisomerase I, also formed stable complexes with PEG-PLL but exhibited no sensitivity to S1 nuclease (data not shown). Additionally, a complex with linear plasmid DNA, prepared by treatment with a restriction enzyme (EcoRI) having a unique recognition site on the plasmid, was smoothly degraded to oligo-DNA pieces in a nonspecific manner (data not shown). The observed differences in S1 nuclease sensitivity to plasmid isomer constructs suggest that topological features of the block copolymer–DNA supramolecular complex influence the enzymatic fragmentation process.

Polyion complex formation between DNA and cationic compounds is known to induce a coil–globule transition, thereby resulting in condensed complexes with ordered morphologies, mainly in toroidal or rod-like forms.[14–18] Consistent with this, charge-neutralizing DNA complexation with PEG-PLL produces a detectable transition from an expanded DNA superhelix into a compact state, as confirmed by static and dynamic light scattering[13] as well as by direct observation with fluorescence microscopy.[18] Although the structural details of the condensed plasmid in this complex have not yet been clarified, significant structural features are probably present in the supercoiled double-stranded DNA upon polyion-induced condensation. Constrained structural order (or regular disorder) in the double-stranded DNA structure might be regularly repeated in this polyion-induced condensation process. This would permit the DNA to adopt particular structures that compensate for the structural constraints accompanying conformation transitions during complexation. Consequently, these specific disordered sites in the condensed DNA strands may preferentially promote S1 nuclease attack, thereby resulting in the observed regular DNA fragmentation.

Supercoiled DNA associated with poly(L-lysine) homopolymer with degrees of polymerization (DP) of 19 and 260 exhibited only nonspecific S1 nuclease degradation without any ordered cleavage, as shown by a smeared electrophoresis gel stain (data not shown). This indicates that polyion complexation alone is not sufficient and that the PEG segment in the block copolymer plays a crucial role in regulating the nuclease sensitivity in addition to promoting the complex solution stability. Inter- or intramolecular steric repulsion of hydrated PEG segments may contribute to the modulated structure of plasmid DNA.

The sensitivity of single-strand-cleavage endonucleases like S1 nuclease against naked plasmid DNAs has been investigated since the 1980s.[19–22] The naked DNAs are first nicked and then linearized. The cleavage sites are cruciform loops, which are adopted by short inverted repeat (palindrome) sequences in the topologically stressed double helix.

Formation of the hairpin-loop structure relieves the topological strain in double-stranded circular DNA molecules. These inverted repeats, separated by nonrepetitious sections of DNA, are specifically cleaved by single-strand-specific nucleases at the center of each hairpin loop. Torsional stress of negative supercoiling of plasmid DNA occasionally induces a kink in the DNA strand with an acute angle. The high susceptibility of palindrome sequences to S1 nuclease digestion led us to assume that the regular fragmentation seen here in the system with the PEG-PLL/plasmid DNA (pDNA) complex might be a result of selective digestion at the cruciform loop regularly induced in the condensed DNA strands. To get an insight into this assumed mechanism, inverted repeats larger than five continuous sequences are picked up from three plasmids (pBR322, pGL3-Luc, and ColE1) by using computer analysis.[23] Neighboring smaller palindromes separated by one or two nonrepetitious sections of DNA were also taken into consideration. It is to be expected that hairpin stability will be directly proportional to stem length but inversely proportional to loop length. The inverted sequences were marked from four to one according to the hairpin stability, as summarized in Figure 2a as a function of base number. Obviously, there are quite a few palindrome sequences. Denaturation of the DNA double strand is necessary for transformation from the normal interstrand base pairing to the intrastrand base pairing of the cruciform structure. The binding energy of the A–T (adenine–thymine) pair is lower than that of the G–C (guanine–cytosine) pair, because two hydrogen bonds are contributing to the pairing between A and T while three contribute between G and C. Thus, the composition of A–T pairs within the palindrome sequences was also examined (Figure 2b). Refinement according to palindrome size and A–T composition allowed the extraction of several sites as candidates for S1 nuclease recognition; these are indicated as dotted lines in Figure 2a and b and as slashes in the pDNA maps (Figure 2d). By use of these refined sites, combinations satisfying the regular fragments were surveyed by consideration of fragment lengths, since two sites on the circular plasmid DNA must be cleaved (for example, 3/12+9/12 = 12/12). Consequently, combinations of cleavage sites yielding the seven DNA sizes were acquired for all three plasmid DNAs

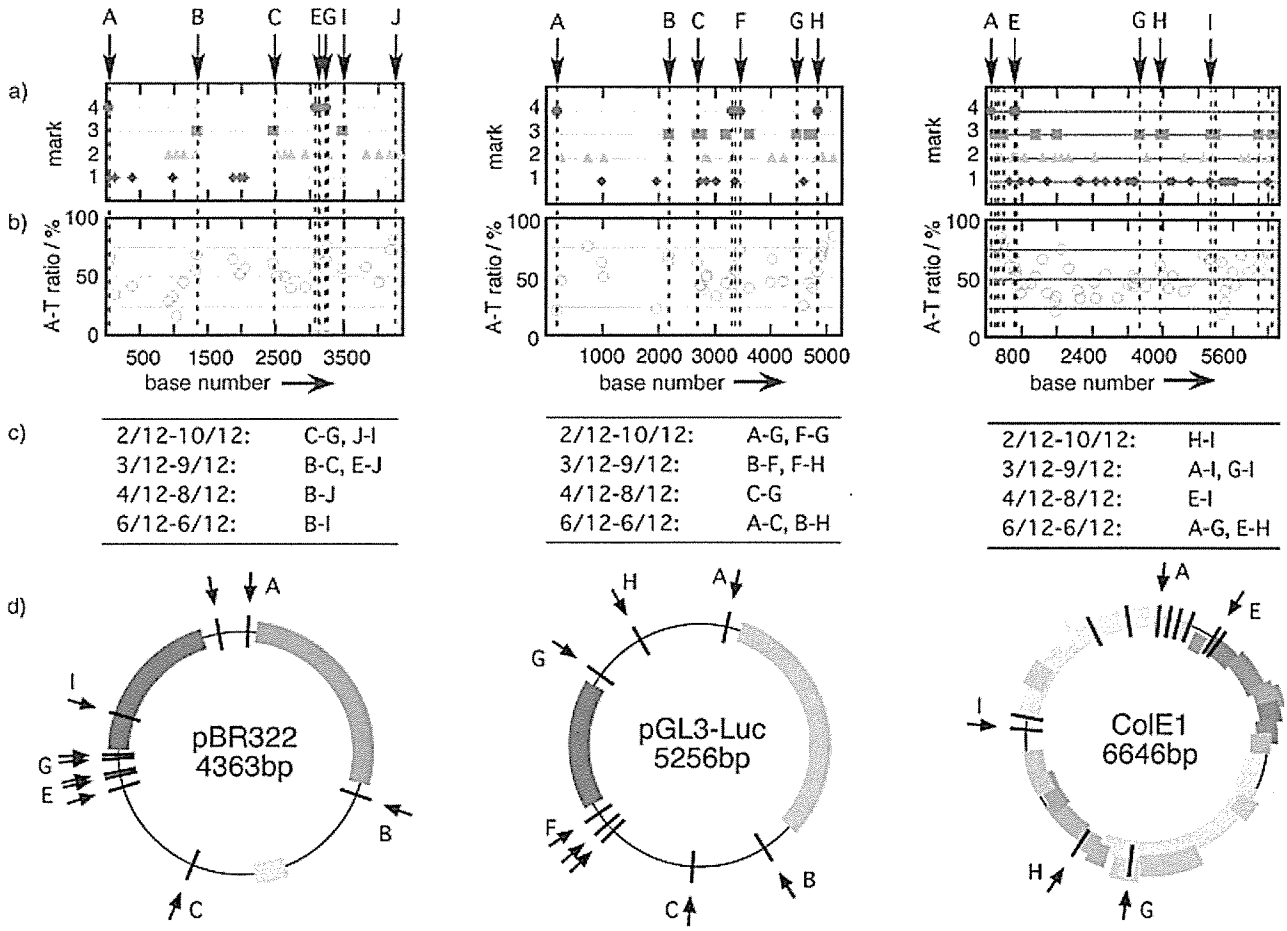

Figure 2. Palindrome maps and protein codes of the three plasmid DNAs pBR322 (left), pGL3-Luc (middle), and ColE1 (right). a) Cruciform stability by the size of inverted repeats. Higher mark numbers indicate higher cruciform stability. b) Percentage A–T composition in the considered palindrome sequences as a function of base number in the plasmid DNAs. Here, base 1 was defined as the recognition site of the EcoR1 restriction enzyme. The dotted lines in panels (a) and (b) indicate refined digestion sites as evaluated from the panels. The combinations of cleavage sites that satisfy the seven-piece fragmentation pattern are summarized in (c). Those evaluated cleavage sites are shown as arrows with capital letters in panels (a) and (d); in addition, correlation between the protein-coding regions and proposed cleavage sites is shown in (d).

(listed in Figure 2c) and those sites are indicated as arrows in Figure 2a and d. The regular fragmentation can be explained by assuming that the cruciform structures regularly induced in the DNA by complexation with the PEG-PLL block copolymer are digested by the single-strand-recognition endonuclease.

Obviously, development of the extruded cruciform structure requires definite stress. The cruciform formation in the naked pDNA is known to be driven by the torsional stress of negative supercoiling.[22] In the complex of pDNA with PEG-PLL, the stress of condensation by the polycation further amplified the torsional stress of the supercoiled conformation, so that the cruciform may be developed in multiple sites. It should be noted that the charge ratio of 1.0 is indeed a critical point in the pDNA transition from extended state to condensed state. The ethidium bromide exclusion assay showed an abrupt decrease in the relative fluorescence, which indicates condensation of DNA molecules, at a charge ratio range of around 1.0 (see the Supporting Information). Additionally, the transition of DNA shape is confirmed by direct observation with atomic force microscopy (Figure 3). Apparently, complex shapes at the charge ratio of 1.0 comprise preferentially condensed rod and toroid conformations.

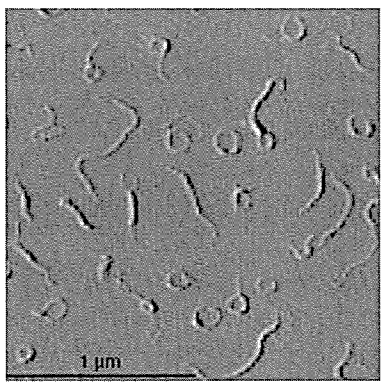

Figure 3. AFM image of plasmid DNA (pGL3-Luc) complexed with the PEG-PLL block copolymer at a charge ratio of 1.0. The image was taken in the amplitude mode for the complex after equilibration in solution for 24 hours. A scale bar is included in the figure.

Furthermore, the potential cleavage site (palindrome site) and protein-coding region have a very interesting correlation, in that the former is located just outside of the latter, as can be clearly seen in Figure 2d. It is worth mentioning that this is commonly observed among the three examined plasmids. This correlation is most distinctive in the ColE1 plasmid, which has various protein codes (Figure 2d). The fact that the selected inverted repeats are located just in the gap or at the terminus of various coding regions suggests that the cruciform structure may substantially contribute to the regulation of gene expression[21] and is most likely to be a landmark for DNA-binding proteins. It should be noted that hypersensitivity of structured DNA to S1 nuclease has been observed in regions of transcriptionally active genes in chromatin.[24] DNA breakage by S1 nuclease is observed in apoptotic cells[25] and also more in mitotic chromosomes than chromosomes in interphase cells.[26] This may be a reflection of the differences of stress under such circumstances. The cruciform structural motifs must be to regulate the binding of proteins, nucleases, promoters, or transcription factors; the full function remains to be determined. Yet, the potential for designing synthetic polymer constructs that reliably alter or mimic these supramolecular structures or for imparting new features of molecular recognition by using the materials of unconventional biopolymer complexes, as demonstrated here, is exciting.

In conclusion, we have demonstrated that the size-specific cleavage of plasmid DNA by S1 nuclease can be mediated by condensed complexes of plasmids with synthetic block copolymers without any sequence-specific binding. The recognition site is probably the cruciform structure induced by DNA complexation with the block copolymer. This means that DNA inherently retains sequences that can transform its secondary structure by certain stimuli and the synthetic polymer reveals the functional structure by complexation. The observed unique sensitivity of PEG-PLL/pDNA complexes to S1 nuclease should provide an insight into the mechanisms of endogenous protein-induced modification of DNA and into the design of artificial restriction enzymes and gene-exploring systems through supramolecular assembly of synthetic macromolecular materials.

Received: January 19, 2005
Published online: May 4, 2005

Keywords: block copolymers · DNA cleavage · hydrolases · molecular recognition · self-assembly

[1] J.-M. Lehn, *Science* **2002**, *295*, 2400–2403.
[2] G. M. Whitesides, B. Grzybowski, *Science* **2002**, *295*, 2418–2421.
[3] J. D. Hartgerink, E. Beniash, S. I. Stupp, *Science* **2001**, *294*, 1684–1688.
[4] D. E. Discher, A. Eisenberg, *Science* **2002**, *297*, 967–973.
[5] S. Jain, F. S. Bates, *Science* **2003**, *300*, 460–464.
[6] A. Harada, K. Kataoka, *Science* **1999**, *283*, 65–67.
[7] J. N. Cha, G. D. Stucky, D. E. Morse, T. J. Deming, *Nature* **2000**, *403*, 289–292.
[8] J. A. Hubbell, *Science* **2003**, *300*, 595–596.
[9] R. Savic, L. Luo, A. Eisenberg, D. Maysinger, *Science* **2003**, *300*, 615–618.
[10] A. V. Kabanov, V. A. Kabanov, *Adv. Drug Delivery Rev.* **1998**, *30*, 49.
[11] S. Katayose, K. Kataoka, *Bioconjugate Chem.* **1997**, *8*, 702–707.
[12] S. Katayose, K. Kataoka, *J. Pharm. Sci.* **1998**, *87*, 160–163.
[13] K. Itaka, K. Yamauchi, A. Harada, K. Nakamura, H. Kawaguchi, K. Kataoka, *Biomaterials* **2003**, *24*, 4495–4506.
[14] K. Miyata, Y. Kakizawa, N. Nishiyama, A. Harada, Y. Yamasaki, H. Koyama, K. Kataoka, *J. Am. Chem. Soc.* **2004**, *126*, 2355–2361.
[15] U. K. Laemmli, *Proc. Natl. Acad. Sci. USA* **1975**, *72*, 4288–4292.
[16] S. M. Mel'nikov, V. G. Sergeyev, K. Yoshikawa, *J. Am. Chem. Soc.* **1995**, *117*, 9951–9956.
[17] J. Rackstraw, A. L. Martin, S. Stolnik, C. J. Roberts, M. C. Garnett, M. C. Davies, S. J. B. Tendler, *Langmuir* **2001**, *17*, 3185–3193.
[18] Y. Yamasaki, S. Katayose, K. Kataoka, K. Yoshikawa, *Macromolecules* **2003**, *36*, 6276–6279.

[19] D. M. J. Lilley, *Nucleic Acids Res.* **1981**, *9*, 1271–1289.
[20] N. Panayotatos, R. D. Wells, *Nature* **1981**, *289*, 466–470.
[21] U. R. Mueller, W. M. Fitch, *Nature* **1982**, *298*, 582–585.
[22] M. Gellert, M. H. O'Dea, K. Mizuuchi, *Proc. Natl. Acad. Sci. USA* **1983**, *80*, 5545–5549.
[23] Palindrome sequence analyses were performed on a Macintosh iBook 400 MHz computer by using the FROG-Mac program (written by N. Miki at Osaka University and available from http://pharma1.med.osaka-u.ac.jp/freeware.html).
[24] A. Larsen, H. Weintraub, *Cell* **1982**, *29*, 609–622.
[25] M. C. Peitsch, C. Mueller, J. Tschopp, *Nucleic Acids Res.* **1993**, *21*, 4206–4209.
[26] G. Juan, W. Pan, Z. Darzynkiewicz, *Exp. Cell Res.* **1996**, *227*, 197–202.

CHEMBIOCHEM

Smart Polyion Complex Micelles for Targeted Intracellular Delivery of PEGylated Antisense Oligonucleotides Containing Acid-Labile Linkages

Motoi Oishi,[a] Fumi Nagatsugi,[b] Shigeki Sasaki,[b] Yukio Nagasaki,*[a, d] and Kazunori Kataoka*[c]

A novel pH-sensitive and targetable antisense ODN delivery system based on multimolecular assembly into polyion complex (PIC) micelles of poly(L-lysine) (PLL) and a lactosylated poly(ethylene glycol)–antisense ODN conjugate (Lac-PEG–ODN) containing an acid-labile linkage (β-propionate) between the PEG and ODN segments has been developed. The PIC micelles thus prepared had clustered lactose moieties on their peripheries and achieved a significant antisense effect against luciferase gene expression in HuH-7 cells (hepatoma cells), far more efficiently than that produced by the nonmicelle systems (ODN and Lac-PEG–ODN) alone, as well as by the lactose-free PIC micelle. In line with this pronounced antisense effect, the lactosylated PIC micelles showed better uptake than the lactose-free PIC micelles into HuH-7 cells; this suggested the involvement of an asialoglycoprotein (ASGP) receptor-mediated endocytosis process. Furthermore, a significant decrease in the antisense effect (27% inhibition) was observed for a lactosylated PIC micelle without an acid-labile linkage (thiomaleimide linkage); this suggested the release of the active (free) antisense ODN molecules into the cellular interior in response to the pH decrease in the endosomal compartment is a key process in the antisense effect. Use of branched poly(ethylenimine) (B-PEI) instead of the PLL for PIC micellization led to a substantial decrease in the antisense effect, probably due to the buffer effect of the B-PEI in the endosome compartment, preventing the cleavage of the acid-labile linkage in the conjugate. The approach reported here is expected to be useful for the construction of smart intracellular delivery systems for antisense ODNs with therapeutic value.

Introduction

Antisense oligodeoxynucleotides (ODNs) have attracted much attention as a class of therapeutic agents that can be used to target mRNA for specific inhibition of gene expression.[1] Nevertheless, the therapeutic value of antisense ODNs under in vivo conditions has not been fully proven to be effective owing to several obstacles, including nonspecific interaction with plasma protein,[2] low stability against enzymatic degradation,[3] low permeability across the cell membrane,[4] and preferential liver and renal clearance.[3] Therefore, a high dose of the antisense ODN is generally required to achieve a significant antisense effect in vivo. To obtain the desired antisense effect, a variety of antisense ODN delivery systems such as cationic lipids (lipoplexes)[5] and cationic polymers (polyplexes)[6] have been developed, and some of these systems contribute substantially to ODN stability against enzymatic degradation and increased cellular uptake, at least under in vitro conditions. However, due to the nonspecific nature of interactions of cationic components with negatively charged biomacromolecules, they often tend to show nonspecific disposition characteristics and short circulating lifetimes in the blood after systemic injection.[7] Recently, a new class of antisense ODN delivery systems has emerged based on polyion complex (PIC) micelles composed of PEG–polycation block copolymers (PEG = poly(ethylene glycol)) and oppositely charged antisense ODNs, held together by electrostatic interactions.[8] The PIC micelles exhibited excellent solubility in aqueous media, high tolerance of entrapped ODNs against enzymatic degradation, and minimal interaction with negatively charged biomacromolecules and cell membrane, owing to the steric stabilization of the very dense PEG corona surrounding the PIC core. However, electrostatic

[a] *Dr. M. Oishi, Prof. Dr. Y. Nagasaki*
Department of Materials Science and Technology
Tokyo University of Science
2641 Yamazaki, Noda, Chiba 278-8510 (Japan)
Fax: (+81) 4-7123-8878
E-mail: nagasaki@ims.tsukuba.ac.jp

[b] *Prof. Dr. F. Nagatsugi, Prof. Dr. S. Sasaki*
Graduate School of Pharmaceutical Science
Kyushu University
3-3-1 Maidashi, Higashi-ku, Fukuoka 812-8582 (Japan)

[c] *Prof. Dr. K. Kataoka*
Department of Materials Science and Engineering
Graduate School of Engineering, The University of Tokyo
7-3-1 Hongo, Bunkyo-ku, Tokyo 113-8656 (Japan)
Fax: (+81) 3-5841-7139
E-mail: kataoka@bmw.t.u-tokyo.ac.jp

[d] *Prof. Dr. Y. Nagasaki*
Current address:
Tsukuba Research Center for Interdisciplinary Materials Science
University of Tsukuba, Tsukuba 305-8573 (Japan)

  DOI: 10.1002/cbic.200400334

interaction between PEG–polycation block copolymer and antisense ODN seems to be weak under extremely dilute conditions, due to the low molecular weight of the antisense ODN, with this often leading to the dissociation of the PIC micelles below the critical association concentration (cac). Therefore, the stability of the PIC micelles used for entrapping the antisense ODNs needs to be further improved for use in systemic ODN delivery. On the other hand, the smooth and efficient release of entrapped antisense ODNs from PIC micelles into the intracellular environment after their trafficking into the target cells is needed to achieve an antisense effect.

Recently, our group[9] and Park et al.[10] have independently reported novel PIC micelles composed of an alternative combination of an anionic PEG–ODN conjugate bearing an acid-labile linkage between the PEG and the antisense ODN segment and a polycation of appreciable molecular weight. Improved stability of the PIC micelles is to be expected from this approach, due to the increased association force of the entrapped polycations of appreciable molecular weight. In addition to showing resistance against enzymatic degradation and minimal interaction with negatively charged biomacromolecules, the PEG–ODN/polycation PIC micelles underwent cleavage of the acid-labile linkages between PEG and antisense ODN segments in response to the endosomal pH, which is known to be 1.4–2.4 units lower than that found under standard physiological conditions.[11] The detachment process of the PEG segment in response to the pH decrease in the endosomal compartment would be expected to correspond to the transport of the free (active) antisense ODN moiety from endosome to cytoplasm. Nevertheless, PEG–ODN/polycation PIC micelles may show reduced cellular uptake due to limited interaction between the PEG shell of the micelle and the cell membrane, so installation of specific ligand molecules on the surfaces of the PEG–ODN/polycation PIC micelles is indispensable in order to achieve specific and enhanced cellular uptake through receptor-mediated endocytosis, allowing the effective dose of antisense ODN to be reduced.

Here we wish to report the preparation and bioactivity of pH-sensitive lactosylated PIC micelles composed of a lactosylated PEG–ODN conjugate (Lac-PEG-ODN) bearing an acid-labile linkage between PEG and ODN segments and poly(L-lysine) (PLL), as shown in Figure 1. The lactose moieties on the surfaces of the PIC micelles act as a specific ligand for hepatocytes (liver cells), because hepatocytes are known to have an abundance of asialoglycoprotein (ASGP) receptors that recognize and internalize glycoproteins bearing terminal lactose moieties.[12] The lactosylated PIC micelles could potentially be expected to show enhanced antisense effects relative to PIC micelles without lactose moieties, due to the enhancement of cellular uptake through ASGP receptor-mediated endocytosis.

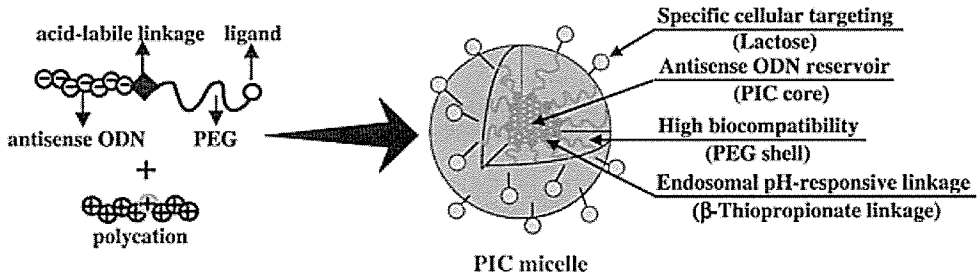

Figure 1. Illustration of the PIC micelle.

Results and Discussion

Synthesis of the lactosylated poly(ethylene glycol)–oligodeoxynucleotide (Lac-PEG-ODN) conjugate

A synthetic route to Lac-PEG-ODN conjugate is shown in Scheme 1. A heterobifunctional PEG bearing an allyl group at the α-end and a hydroxy group at the ω-end (Ally-PEG-OH) was synthesized by anionic ring-opening polymerization of ethylene oxide with use of the allyl alcohol/potassium/naphthalene initiator system.[13] The radical addition of 3-mercaptopropionic acid to the Allyl-PEG-OH in the presence of AIBN quantitatively afforded a carboxylic acid-PEG-OH (HOOC-PEG-OH), which was in turn converted into a HOOC-PEG-Acrylate by treatment with acryloyl chloride in the presence of triethylamine. According to SEC and ^{1}H NMR analyses (Figure 2), the molecular weight of the HOOC-PEG-Acrylate (SEC: $M_n = 4450$, $M_w/M_n = 1.04$ and ^{1}H NMR: $M_n = 4630$) agrees with the calculated molecular weight (calcd. $M_n = 5060$), and a carboxylic acid group and an acrylate group were shown to have been quantitatively introduced at the α-end and the ω-end of the PEG, respectively. The quantitative introduction of a lactose group at the carboxylic acid end of the HOOC-PEG-Acrylate was also performed by treatment with excess 4-aminophenyl β-D-lactopyranoside in the presence of 1-ethyl-3-(3-dimethylaminopropyl)carbodiimide hydrochloride (EDC) and *N*-hydroxysuccinimide (NHS). A ^{1}H NMR spectrum of the Lac-PEG-Acrylate is shown in Figure 3 with assignments, the peaks of aromatic residue assignable to 4-aminophenyl β-D-lactopyranoside moiety being clearly observable at $\delta = 7.14$ and 7.34 ppm, along with the acrylate peaks at $\delta = 5.83$–6.54 ppm. From the integral ratios between aromatic peaks and acrylate peaks or PEG backbone peaks at 3.65 ppm, it was confirmed that the lactose moiety had been quantitatively introduced at the PEG end. To obtain a Lac-PEG-ODN conjugate bearing an acid-labile linkage (β-thiopropionate linkage), a Michael reaction between the 3′-thiol-modified antisense ODN (5′-ATG CCC ATA CTG TTG AG–$CH_2CH_2CH_2SH$, firefly luciferase, pGL3-control antisense sequence[14]) and excess Lac-PEG-Acrylate (10 equiv) was carried out according to our previous report.[9] For the controls, Ace-PEG-ODN conjugate bearing an acetal group at the PEG end and Lac-PEG-scrODN conjugate bearing a scrambled ODN sequence were also synthesized. Furthermore, a Lac-PEG-Mal-ODN conjugate with no acid-labile linkage between PEG and ODN segments was synthesized through a Michael reaction between Lac-PEG-Maleimide and the 3′-thiol-modified ODN, as shown in Scheme 1.

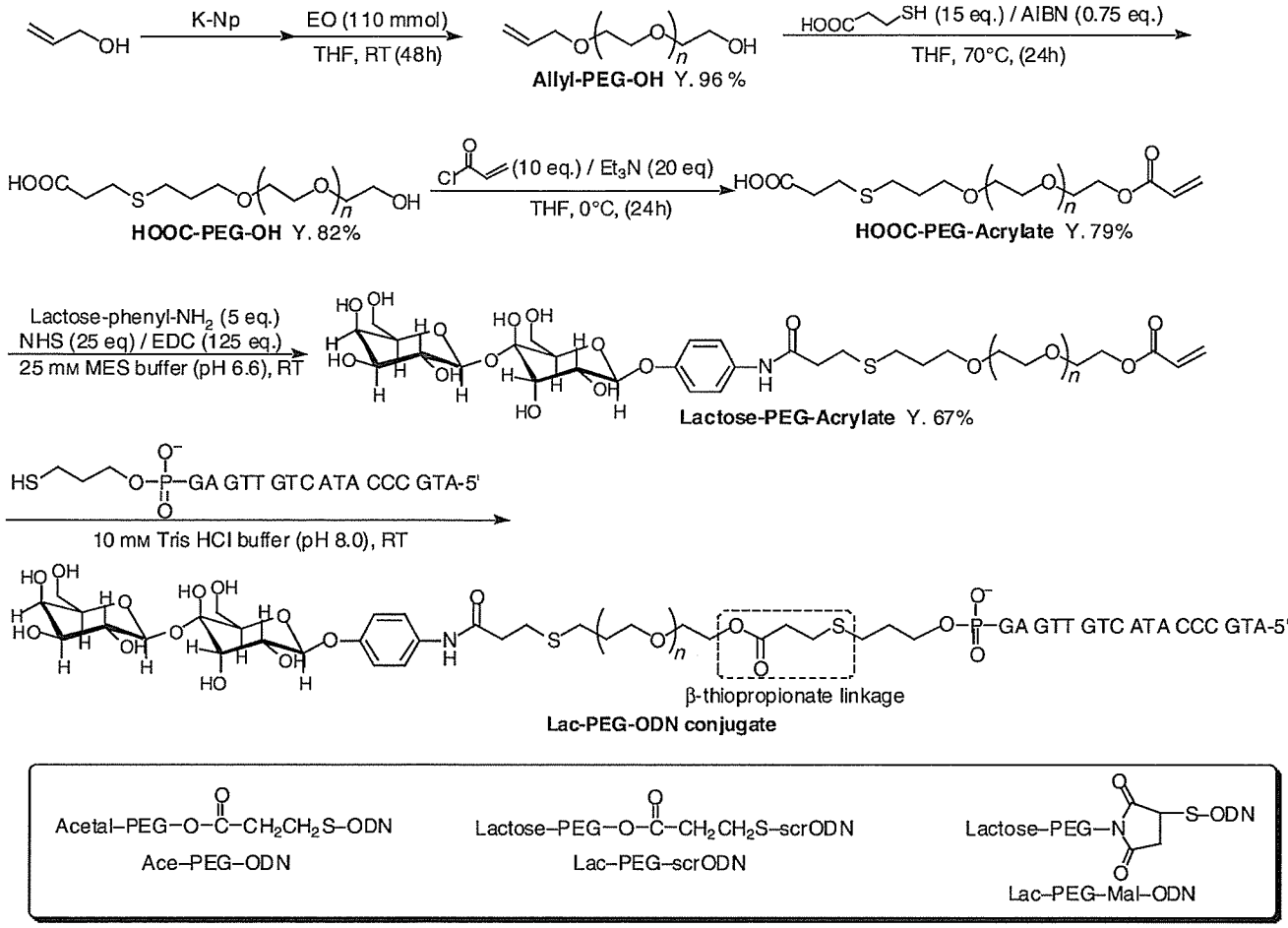

Scheme 1. Synthetic route to Lac-PEG-ODN.

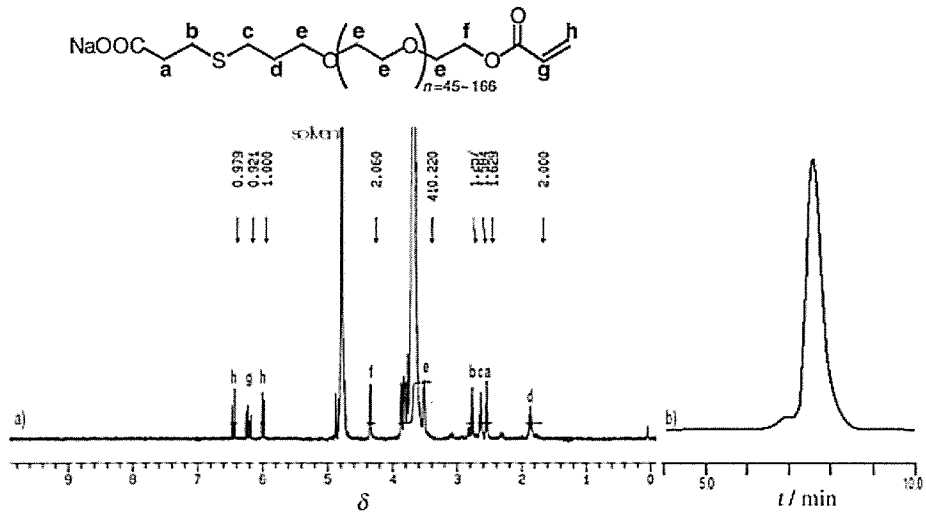

Figure 2. a) ^{1}H NMR spectrum, and b) SEC chromatogram of HOOC-PEG–acrylate.

Cellular association and internalization of the PIC micelles

The obtained Lac-PEG-ODN conjugate would be expected to form a PIC micelle through electrostatic interaction on mixing with the appropriate polycation, as illustrated in Figure 1. ω-FITC-labeled (FITC = fluorescein isothiocyanate) Lac-PEG-ODN conjugate and ω-FITC-labeled Ace-PEG-ODN conjugate were separately mixed with PLL (degree of polymerization (DP) = 460, M_w = 75 900) with an equal unit molar ratio of the phosphate group in the PEG–ODN conjugate and amino group in PLL (N/P = 1) to form the FITC-labeled PIC micelles. The fluorescence from the Lac-PEG-ODN-FITC/PLL PIC micelles and Ace-PEG-ODN-FITC/PLL PIC micelles was viewed under a fluorescence microscope at different time intervals (30 and 120 min) after their addition to cultured HuH-7 cells in the presence of 10% fetal bovine serum (FBS) (Figure 4). Note that HuH-7 cells express quite a few ASGP receptors that recognize and internalize compounds bearing terminal lactose moieties. The association of the Lac-PEG-ODN-FITC/PLL PIC micelles with the HuH-7 cells and their internalization were observed as early as after 30 min of incubation, and

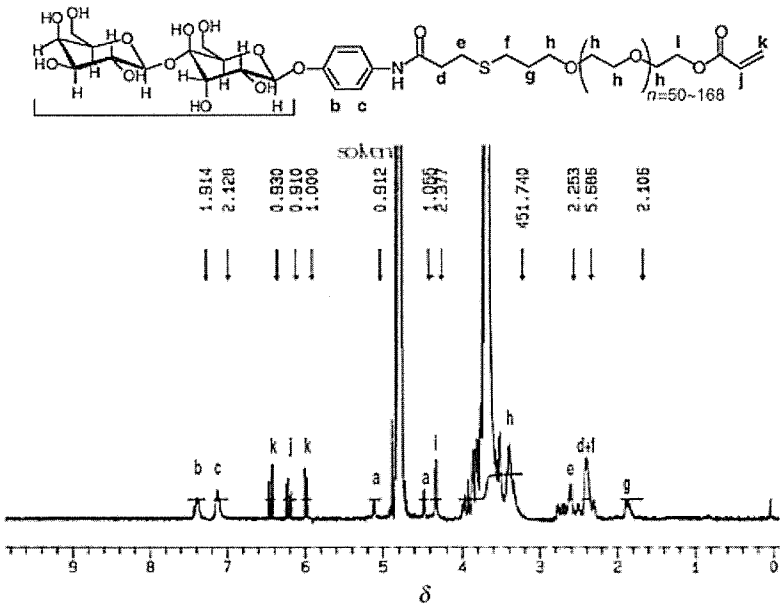

Figure 3. ^1H *NMR spectrum of lactose-PEG–acrylate.*

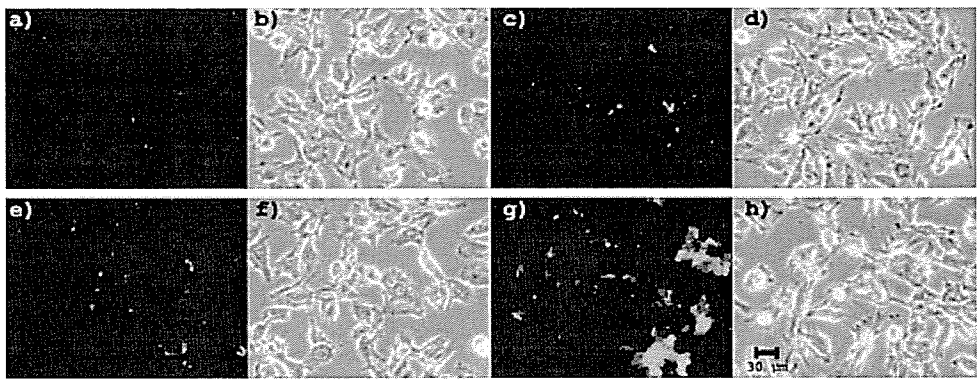

Figure 4. Association and internalization of the Ace-PEG-ODN-FITC/PLL PIC micelles (N/P = 1) and Lac-PEG-ODN-FITC/PLL PIC micelles (N/P = 1) in HuH-7 cells after 30 or 120 min incubation. The PIC micelles used and the incubation time were as follows: a), b) Ace-PEG-ODN-FITC/PLL PIC micelle, 30 min. c), d) Ace-PEG-ODN-FITC/PLL PIC micelle, 120 min. e), f) Lac-PEG-ODN-FITC/PLL PIC micelle, 30 min. g), h) Lac-PEG-ODN-FITC/PLL PIC micelle, 120 min. a, c, e, and g are fluorescent images, and b, d, f, and h are phase-contrast images.

furthermore, the number of fluorescence staining cells and the fluorescence intensity of each staining cell increased with prolongation of incubation time from 30 min to 120 min (26%→ 49% fluorescence positive cells). In contrast, low cellular association of Ace-PEG-ODN-FITC/PLL PIC micelles with HuH-7 cells and low internalization into them was observed even at 120 min (21% fluorescence-positive cells). This result strongly suggests that cellular association and internalization of a Lac-PEG-ODN-FITC/PLL PIC micelle may occur by an ASGP receptor-mediated process, whereas Ace-PEG-ODN-FITC/PLL PIC micelles are taken up into cells only by fluid-phase endocytosis, known to be a substantially slower process than receptor-mediated endocytosis.[15]

Antisense activity of the PIC micelles evaluated by dual luciferase reporter assay

To evaluate the antisense efficiency of the Lac-PEG-ODN in the PIC micelle delivery system, we carried out a dual luciferase reporter assay in HuH-7 cells. Open and closed bars in Figure 5 show the antisense effects of Ace-PEG-ODN/PLL and Lac-PEG-ODN/PLL PIC micelles (N/P = 1, PLL; DP = 460, M_w = 75 900), respectively, in the presence of 10% FBS as a function of the concentration of the conjugate. As the conjugate concentration increases, firefly luciferase expression of the cells treated with Ace-PEG-ODN/PLL PIC micelles or Lac-PEG-ODN/PLL micelles was progressively reduced in dose-dependent manner ($^*P < 0.05$). It was also noticed that the antisense effect of the Lac-PEG-ODN/PLL PIC micelles was approximately 1.5 times higher than that of Ace-PEG-ODN/PLL micelles at 5 and 10 μM ($^*P < 0.05$). When asialofetuin (ASF), a natural glycoprotein ligand for the ASGP receptor, was preincubated with the cells (10 mg mL^{-1}) for 30 min before the addition of the Lac-PEG-ODN/PLL PIC micelle, the antisense effect was reduced significantly even at 10 μM: from 65% inhibition to 38% inhibition (hatched bar 1), the same level as achieved by Ace-PEG-ODN/PLL micelles. Since the ASF is known to act as an inhibitor of ASGP receptor-mediated endocytosis,[16] it is likely that an appreciable fraction of the Lac-PEG-ODN/PLL PIC micelle may be taken up into HuH-7 cells by an ASGP receptor-mediated endocytosis process to achieve pronounced antisense activity in relation to that produced by Ace-PEG-ODN/PLL micelles without any particular affinity toward cellular receptors.

It is worth noting that no reduction in firefly luciferase expression was observed even at 10 μM for Lac-PEG-scrODN/PLL PIC micelle (hatched bar 4), a micelle containing a conjugate of scrambled ODN sequence, indicating that inhibition of firefly luciferase expression by the Lac-PEG-ODN/PLL PIC micelles is indeed a sequence-specific event. Non-micelle systems—the 3′-unmodified antisense ODN alone (hatched bar 2) and Lac-PEG-ODN conjugate alone (hatched bar 3)—failed to inhibit the firefly luciferase expression even at high concentrations (up to 10 μM). This may be explained either by a much more rapid enzymatic degradation of antisense ODN and PEG–ODN conjugate in the medium, relative to the PIC micelle,[9] or by impaired diffusivity of naked antisense ODN and Lac-PEG-ODN conjugate, with their negatively charged and hydrophilic characters, through the nega-

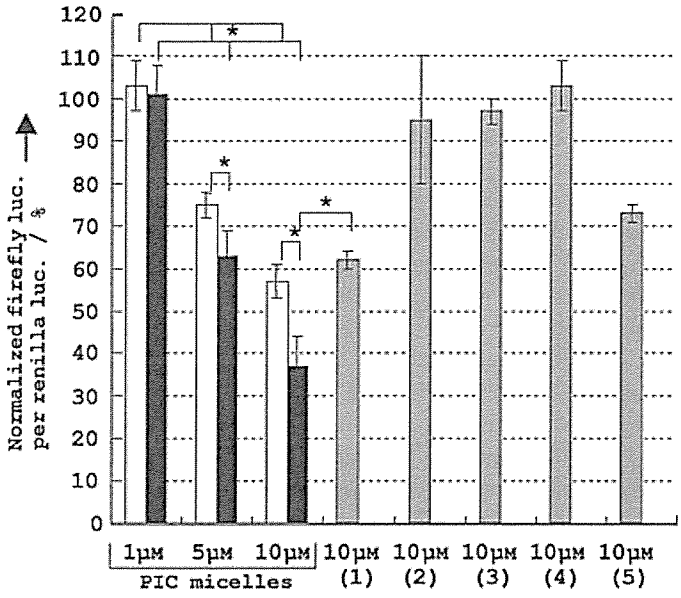

Figure 5. Antisense effects against firefly luciferase gene expression in cultured HuH-7 cells. Open and closed bars show results for the Ace-PEG-ODN/PLL PIC micelles and the Lac-PEG-ODN/PLL PIC micelles, respectively, at varying concentrations. Hatched bars are results for: 1) Lac-PEG-ODN/PLL PIC micelle at 10 μM with ASF, 2) antisense ODN alone at 10 μM, 3) Lac-PEG-ODN conjugate alone at 10 μM, 4) Lac-PEG-scrODN/PLL PIC micelle at 10 μM, and 5) Lac-PEG-Mal-ODN/PLL PIC micelle at 10 μM. Normalized ratios between the firefly luciferase activity (firefly luc.) and the renilla luciferase activity (renilla luc.) are shown in the ordinate. The indicated concentrations of conjugate and antisense ODN were the final concentrations in the total transfection volume (250 μL). The data are shown as the averages from triplicate experiments ±SD. P < 0.05.*

tively charged cell membrane. It should also be noted that the Lac-PEG-Mal-ODN/PLL micelle, a micelle containing the conjugate with a non-acid-labile linkage,[17] was less effective than the Lac-PEG-ODN/PLL PIC micelle: the former showed 27% inhibition (hatched bar 5), whereas the latter achieved 65% inhibition at 10 μM (closed bar). The significant difference in antisense effects between Lac-PEG-ODN/PLL PIC micelle and Lac-PEG-Mal-ODN/PLL PIC micelle can be ascribed to the difference in the natures of their linkages between PEG and ODN segments. The Lac-PEG-ODN conjugate contains an acid-labile (β-thiopropionate) linkage that is cleavable in the low-pH endosome environment, provoking the release of hundreds of free PEG strands from the PIC micelle to increase the colloidal osmotic pressure within the endosomal compartment,[18] and eventually to induce the swelling and disruption of the endosome. This event may facilitate the transport of free antisense ODN into cytoplasm. On the other hand, the Lac-PEG-Mal-ODN conjugate, bearing a stable thiomaleimide linkage not cleavable in the endosomal compartment, may have no contribution in facilitating endosomal escape through osmotic pressure increase. Furthermore, the presence of PEG strands may restrict the interaction of ODN segments with target mRNA in cytoplasm through steric hindrance, as observed by Moulton et al. for conjugates of antisense phosphorodiamidate morpholino oligomers with peptide.[19] These results indicate that the design of the engineered linkage with programmed sensitivity toward intracellular environment ("smart" PEGylation) is of importance in the successful delivery of the PEG-antisense ODN conjugate.

The effect of the PLL length on the antisense activity of the PIC micelles

The effect of the PLL length (DP) on the antisense effect of the PIC micelles was then examined by comparing PLLs with varying DPs (40, 100, and 460). As can be seen in Figure 6a, a striking effect of PLL length on antisense efficacy of the PIC micelle was observed: micelles prepared from shorter PLL components (DP = 40, Mw = 8300) showed only limited efficacy at 5 μM antisense ODN with a 24 h incubation period ($^*P < 0.05$) relative to those with longer PLLs (DP = 100, Mw = 20900 and 460,

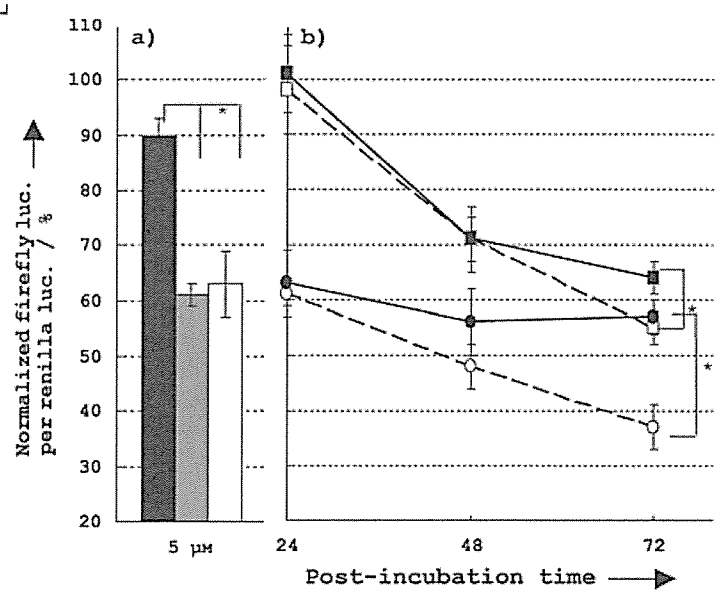

Figure 6. Effect of: a) PLL length (DP = 40 ■, 100 ▪, and 460 □), and b) post-incubation time (24, 48, and 72 h) on the antisense effect of the lactosylated PIC micelles. Normalized ratios between the firefly luc. and the renilla luc. are shown in the ordinate. The final concentrations of conjugate in the total transfection volume (250 μL) were 1 μM (squares) or 5 μM (circles) for DP = 100 (open symbol) or DP = 460 (filled symbol). The data are shown as the averages from triplicate experiments ±SD. P < 0.05.*

Mw = 75900). Presumably the PIC micelles formed from PLL (DP = 40) may be unstable under the extremely dilute conditions ([ODN] ≈ 5 μM) due to the critical dissociation phenomenon, leading to the enzymatic degradation of the Lac-PEG-ODN conjugate. The effect of the incubation time was then further studied for the PIC micelles prepared from the PLLs of DP = 100 and 460. After incubation of HuH-7 cells with PIC micelles for 24 h, the medium was changed to a fresh one free of PIC micelles to continue the culture for a designated time period (24, 48, and 72 h). As can be seen in Figure 6b, both PIC micelles composed of PLL with DP = 100 and DP = 460 (N/P = 1) exhibited an appreciable time-dependent increase in antisense effect even at 1 μM. The antisense effect of the PIC micelle with PLL (DP = 460) reached a constant value after 48 h post-

incubation, whereas that with PLL (DP = 100) exhibited an almost liner increase in antisense effect with the post-incubation time period. Notably, a significant antisense effect was achieved for the PIC micelles with PLL (DP = 100) (45% inhibition at 1 μM and 62% inhibition at 5 μM) after 72 h post-incubation relative to that with PLL (DP = 460) (35% inhibition at 1 μM and 42% inhibition at 5 μM). A lowered antisense effect for the systems with longer PLL (DP = 460) is presumably due to overstabilization of the PIC core, restricting the release of the antisense ODN into the cytoplasm.

The effect of the polycation structure in the PIC core on the antisense activity

To study the effect of the polycation structure in the PIC core on the antisense effects of PIC micelles, branched poly(ethylenimine) (B-PEI, DP = 580, M_w = 25 000) was chosen as the counter polycation, as it has often been used for gene delivery in the form of DNA/B-PEI complexes displaying high transfection efficiency due to the endosomal disruption property of B-PEI (so called "buffer" or "proton-sponge" effect).[20] Nevertheless, the antisense effect of Lac-PEG-ODN/B-PEI PIC micelles (N/P = 1, 9% inhibition at 5 μM and 42% inhibition at 10 μM) was lower than that of Lac-PEG-ODN/PLL micelles (N/P = 1) at 5 and 10 μM ($^*P < 0.05$), as shown in Figure 7. Presumably, the buffer effect of the B-PEI may prohibit the decrease in the endosomal pH,[21] and this should be unfavorable for the cleavage of the acid-labile linkage (β-thiopropionate) of the Lac-PEG-ODN conjugate in the endosome, leading to the release of intact and relatively less active Lac-PEG-ODN conjugate into the cytoplasm.

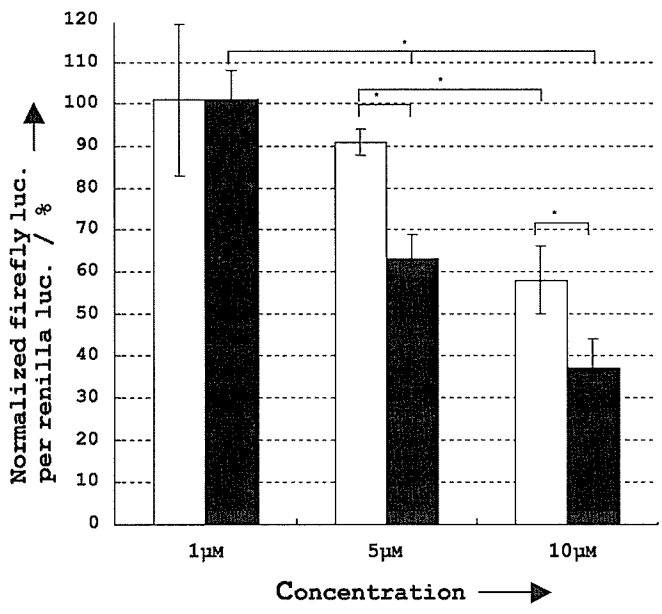

Figure 7. Effect of PIC core polycation structure on the antisense effects of the lactosylated PIC micelles. Normalized ratios between the firefly luc. and the renilla luc. are shown in the ordinate. The indicated concentrations of conjugate were the final concentrations in the total transfection volume (250 μL): □ B-PEI PIC micelles, ■ PLL PIC micelles. The data are shown as the averages from triplicate experiments ± SD. $P^* < 0.05$.

Conclusion

In conclusion, this study reports the preparation of a novel intracellular environment-responsive and targetable antisense ODN delivery system based on the PIC micelle composed of PLL and Lac-PEG-ODN conjugate bearing an acid-labile linkage (β-propionate) between PEG and ODN segments. The lactosylated PIC micelles thus prepared exhibited better association with HuH-7 cells than the lactose-free PIC micelles, as observed by fluorescence microscopy at different time intervals. Delivery of antisense ODN by lactosylated PIC micelle resulted in a significant antisense effect (65% inhibition) for firefly luciferase expression in HuH-7 cells, far more efficient than achieved by using the 3′-unmodified antisense ODN alone (3% inhibition), Lac-PEG-ODN alone (3% inhibition), or lactose-free PIC micelles (45% inhibition), as evaluated by dual luciferase reporter assay. This pronounced antisense effect of the lactosylated PIC micelles indicates that ASGP receptor-mediated endocytosis is considerably involved in the cellular uptake of the lactosylated PIC micelles. Furthermore, a decrease in antisense effect was observed for the lactosylated PIC micelles without any acid-labile linkage (65→27% inhibition), suggesting that cleavage of the acid-labile linkage may occur in response to the lower pH in the endosomal compartment, inducing the efficient release of the active (free) antisense ODN from the PIC core. Such structural parameters—length and type of counter polycation used to make PIC micelles—substantially affected their antisense effects. Significant antisense effects of the PIC micelles (63% inhibition at 5 μM and 45% inhibition at 1 μM) were achieved at 72 h post-incubation time by using PLL with DP = 100, presumably due to the efficient release of antisense ODN from the PIC core through the polyanion exchange reaction in cytoplasm after the detachment of the PEG shell from the PIC micelle in the endosome. All of these results indicate that the system reported here is highly feasible as a smart intracellular delivery system for antisense ODN and related nucleotide compounds for diverse therapeutics.

Experimental Section

Materials: Tetrahydrofuran, ethylene oxide (Sumitomo Seika), allyl alcohol (Wako), triethylamine (Wako), and acryloyl chloride (Wako) were purified by conventional methods. Propan-2-ol, 3-mercaptopropionic acid, 2,2′-azobisisobutyronitrile (AIBN), 1-ethyl-3-(3-dimethylaminopropyl)carbodiimide hydrochloride (EDC), and *N*-hydroxysuccinimide (NHS) were purchased from Wako and were used without further purification. 4-Aminophenyl β-D-lactopyranoside was purchased from Toronto Research Chemicals, Inc. Potassium naphthalene was used as a THF solution, the concentration of which was determined by titration. Water was purified with a Milli-Q apparatus (Millipore). Plasmid DNAs (pDNA) encoding firefly luciferase (pGL3-Control, Promega; 5256 bpa) and renilla luciferase (pRL-TK, Promega; 4045 bpa) were amplified by use of EndoFree Plasmid Maxi or Mega Kits (QIAGEN). The DNA concentration was determined by reading of the absorbance at 260 nm. PLL (DP = 40, M_w = 8300; DP = 100, M_w = 20 900; DP = 460, M_w = 75 900) and B-PEI (DP = 580, M_w = 25 000) were purchased from Sigma and Aldrich, respectively. 3′-Thiol-modified ODNs (5′-ATG CCC ATA CTG TTG AG-$CH_2CH_2CH_2SH$, firefly luciferase, pGL3-control antisense sequence,[14]

and 5′-TCC GTC TAA TGA CGA GT-$CH_2CH_2CH_2SH$, scrambling sequence) were synthesized as in our previous report[9] with a DNA synthesizer (94DNA/RNA Synthesizer, Applied Biosystems).

Polymer analysis: ^{1}H NMR (400 MHz) spectra were obtained in D_2O with a JEOL EX400 spectrometer. Chemical shifts are reported in ppm relative to D_2O ($\delta = 4.79$, ^{1}H). Size exclusion chromatography (SEC) in an organic solvent was performed with a TOSO HLC-8020 apparatus equipped with an internal refractive index (RI) detector (RID-6 A) with a combination of TSK $G4000_{HR}$ and $G3000_{HR}$ columns and THF as the eluent.

Synthesis of HOOC-PEG-OH: Allyl-PEG-OH ($M_n = 4340$, $M_w/M_n = 1.03$) was prepared as in the previous report.[13] Allyl-PEG-OH (4.34 g, 1.0 mmol) was dissolved in anhydrous THF (30 mL), together with 3-mercaptopropionic acid (1.6 g, 15 mmol, 15 equiv) and AIBN (0.123 g, 0.75 mmol, 0.75 equiv), and the resulting mixture was degassed by three freeze–pump–thaw cycles. The radical addition was carried out at 70 °C for 24 h. The polymer was recovered by precipitation in cold propan-2-ol (−15 °C, 2 L) and centrifuged for 45 min at 6000 rpm. Further purification was carried out by dialysis against distilled, deionized water (M_W cutoff 3500), and the product was then freeze-dried to give HOOC-PEG-OH (3.64 g, 82% yield). SEC $M_n = 4330$, $M_w/M_n = 1.04$ (calcd. $M_n = 5010$); ^{1}H NMR (D_2O): $\delta = 1.83$–1.96 (m, 2H; $NaOOCCH_2CH_2$–S–$CH_2CH_2CH_2O$–), 2.57 (t, $J = 7.6$ Hz, 2H; $NaOOCCH_2CH_2$–S–), 2.63 (t, $J = 7.2$ Hz, 2H; $NaOOCCH_2CH_2$–S–$CH_2CH_2CH_2O$–), 2.82 (t, $J = 7.6$ Hz, 2H; $NaOOCCH_2CH_2$–S–), 3.63 ppm (s, 457H; PEG-backbone)

Synthesis of HOOC-PEG-acrylate: A solution of the HOOC-PEG-OH (2.0 g, 0.45 mmol) and Et_3N (0.911 g, 9.0 mmol, 20 equiv) in THF (15 mL) was added dropwise over 1 h at 0 °C to a mixture of acryloyl chloride (0.400 g, 4.5 mmol, 10 equiv) in THF (5.0 mL). The reaction was allowed to proceed at 0 °C for 24 h in the dark. The polymer was recovered by precipitation in cold propan-2-ol (−15 °C, 1 L) and centrifuged for 45 min at 6000 rpm. Further purification was carried out by dialysis against distilled, deionized water (M_W cutoff 3500) and the product was then freeze-dried to give HOOC-PEG-acrylate (1.60 g, 79% yield). SEC $M_n = 4450$, $M_w/M_n = 1.04$ (calcd. $M_n = 5060$); ^{1}H NMR (D_2O, in Figure 2): $\delta = 1.81$–1.94 (m, 2H; $-H_d$), 2.55 (t, $J = 7.6$ Hz, 2H; $-H_a$), 2.63 (t, $J = 7.2$ Hz, 2H; $-H_c$), 2.80 (t, $J = 7.6$ Hz, 2H; $-H_b$), 3.63 (s, 410H; PEG-backbone, $-H_e$), 4.36 (t, $J = 6.4$ Hz, 2H; $-H_f$), 5.98 (dd, $J = 1.8$, 12.8 Hz, 1H; $-H_h$), 6.23 (dd, $J = 12.8$, 25.4 Hz, 1H; $-H_g$), 6.44 (dd, $J = 1.8$, 12.8 Hz, 1H; $-H_h$).

Lactosylation of HOOC-PEG-acrylate: The HOOC-PEG-acrylate (100 mg, 22 μmol) and 4-aminophenyl β-D-lactopyranoside (48 mg, 111 μmol) were dissolved in MES buffer (25 mM, pH 6.6, 5.0 mL) together with EDC (532 mg, 2.78 mmol, 125 equiv) and NHS (64 mg, 555 μmol, 25 equiv). The reaction mixture was stirred at room temperature for 24 h. The polymer was recovered by precipitation in cold propan-2-ol (−15 °C, 200 mL) and centrifuged for 45 min at 6000 rpm. Further purification was carried out by dialysis against distilled, deionized water (M_W cutoff 3500) and the product was then freeze-dried to give lactose-PEG-acrylate (69 mg, 67% yield). SEC $M_n = 4630$, $M_w/M_n = 1.04$ (calcd. $M_n = 5490$); ^{1}H NMR (D_2O, in Figure 3): $\delta = 1.79$–1.95 (m, 2H; $-H_d$), 2.37~2.41 (m, 4H; $-H_d$, $-H_f$), 2.63 (t, $J = 7.2$ Hz, 2H; $-H_e$), 3.65 (s, 452H; PEG-backbone, $-H_h$), 4.37 (t, $J = 6.4$ Hz, 2H; $-H_i$), 4,46~4,54 (m, 1H; $-H_a$), 5.13~5.19 (m 1H; $-H_a$), 5.98 (dd, $J = 1.8$, 12.8 Hz, 1H; $-H_k$), 6.21 (dd, $J = 12.8$, 25.4 Hz, 1H; $-H_j$), 6.43 (dd, $J = 1.8$, 12.8 Hz, 1H; $-H_k$), 7.14 (d, $J = 7.7$ Hz, 2H; $-H_c$), 7.39 ppm (d, $J = 7.7$ Hz, 2H; $-H_b$).

Synthesis of PEG–ODN conjugates: To obtain a Lac-PEG-ODN conjugate bearing an acid-labile linkage, a Michael reaction of the 3′-thiol-modified ODN with excess lactose-PEG-acrylate (10 equiv) was carried out according to our previous report (79% yield).[9] In addition, three types of PEG–ODN conjugate—possessing an acetal group at the PEG end (Ace-PEG-ODN, 84% yield), a scrambled ODN-sequence (Lac-PEG-scrODN, 88% yield), and a non-acid-labile linkage (Lac-PEG-Mal-ODN, 67% yield)—were also synthesized in the same manner. ^{1}H NMR (for Ace-PEG-ODN conjugate, D_2O): $\delta = 1.19$ (t, $J = 9.4$ Hz, 6H; $-OCH_2CH_3$), 1.73 (t, $J = 7.3$ Hz, 2H; $-SCH_2CH_2COO$–), 1.81–2.33 (m, 36H; 2′-methylene + ODN–$CH_2CH_2CH_2S$–), 2.43 (t, $J = 7.3$ Hz, 2H; $-CH_2CH(OEt)_2$), 3.02–3.16 (m, 4H; $-CH_2SCH_2$–) 3.58 (s, 432H; PEG-backbone + ODN–$CH_2CH_2CH_2S$– + $-OCH_2CH_3$), 3.88–3.94 (m, 36H; 4′-methine + $-COOCH_2$–), 4.16 (s, 34H; 5′-methylene), 4.48 ppm (t, $J = 7.3$ Hz, 1H; $-CH_2CH(OEt)_2$). 1′-Methine protons and 3′-methine protons were overlapped by the peak of H_2O (4.79 ppm).

Preparation of PIC micelle: Specific amounts of the PEG–ODN conjugates and polycations were dissolved in Tris-HCl buffer (10 mM, pH 7.4) to prepare the stock solutions. The solutions were filtered through a 0.1 μm filter to remove the dust. The PEG–ODN conjugate stock solution was mixed with polycation stock solution at an equal unit molar ratio of phosphate group in the PEG–ODN conjugate and amino group in the polycation ($N/P = 1$), followed by the addition of Tris-HCl buffer (10 mM, pH 7.4) including NaCl (0.3 M) to adjust the ionic strength of the solution to physiological conditions (0.15 M NaCl). The size and size distribution of the PIC micelle was elucidated by DLS measurements(DLS-7000, Photal, Otsuka Electronics).[9]

Cell culture: HuH-7 human cancer cells derived from a hepatocarcinoma cell line were obtained from the Cell Resource Center for Biomedical Research, Institute of Development, Aging, and Cancer, Tohoku University. The cells were grown in Dulbecco's modified Eagle's medium (DMEM) supplemented with fetal bovine serum (FBS, 10%), penicillin (100 units mL^{-1}), and streptomycin (100 μg mL^{-1}) at 37 °C in a humidified 5% CO_2 atmosphere.

Fluorescence microscopy: FITC-labeled (FITC = fluorescein isothiocyanate) Lac-PEG-ODN and Ace-PEG-ODN conjugates were prepared from 5′-FITC- and 3′-thiol-modified ODN and lactose-PEG-acrylate. HuH-7 cells were seeded at a density of 5×10^5 cells per dish in a 35 mm glass-bottomed dish (Iwaki, Japan) and kept overnight at 37 °C in a 5% CO_2 atmosphere. The Lac-PEG-ODN-FITC/PLL and Ace-PEG-ODN-FITC/PLL PIC micelles ($N/P = 1$, PLL; DP = 460) were added at a conjugate concentration of 1 μM and incubated at 37 °C in a 5% CO_2 atmosphere for the designated time (30 and 120 min). The cells were washed three times with phosphate buffered saline (PBS) and imaged directly in the cell culture medium with an Olympus IX70 and an appropriate filter.

Dual luciferase reporter assay: HuH-7 cells were plated in a 24-well plate (5×10^4 cells per well) to reach about 50% confluence at transfection. The cells were grown for 24 h and the culture medium was changed to OPIMEM I. The cells were co-transfected with two luciferase plasmids (firefly luciferase, pGL3-control and renilla luciferase, pRL-TK) in the presence of LipofectAMINE (Invitrogen). For each well, pGL3 (0.0835 μg) and pRL (0.75 μg) were applied; the final volume was 250 μL per well. The cells were incubated for 4 h, and the transfection medium was then changed to DMEM with FBS (10%, 225 μL per well). The PIC micelle ($N/P = 1$) (25 μL per well) was added to make up a prescribed concentration. After 24 h incubation, the transfection medium was changed to fresh DMEM with FBS (10%), and the cells were further incubated for the designated time (24, 48, and 72 h). The luciferase expression was monitored with the dual luciferase assay kit (Promega) and ARVOSX-1 (Perkin–Elmer).

Acknowledgements

This work was supported by the Core Research for Evolutional Science and Technology (CREST) of the Japan Science and Technology Agency [JST].

Keywords: antisense agents · bioconjugates · micelles · oligonucleotides · poly(ethylene glycol)

[1] a) S. T. Crooke, *Biotechnol. Genet. Eng. Rev.* **1998**, *15*, 121; b) P. D. Cook, *Handb. Exp. Pharmacol.* **1998**, *131*, 51; c) R. Wagner, *Nature* **1994**, *372*, 323; d) C. A. Stein, Y. C. Cheng, *Science* **1993**, *261*, 1004; e) E. Uhlman, A. Peyman, *Chem. Rev.* **1990**, *90*, 543.

[2] C. A. Stein, *Nat. Med.* **1995**, *1*, 1119.

[3] S. Agrawal, J. Temsamani, W. Galbraith, J. Tang, *Clin. Pharmacokinet.* **1995**, *28*, 7.

[4] P. C. Zamecnik, J. Goodchild, Y. Taguchi, P. S. Sarin, *Proc. Natl. Acad. Sci. USA* **1986**, *83*, 4143.

[5] a) M. Carriere, I. Tranchant, P. A. Niore, G. Byk, N. Mignet, V. Escriou, D. Scherman, J. Herscovici, *J. Liposome Res.* **2002**, *12*, 95; b) L. M. C. de Pedroso, S. Simoes, P. Pires, H. Faneca, N. Duzgunes, *Adv. Drug Delivery Rev.* **2001**, *47*, 277; c) A. D. Miller, *Angew. Chem.* **1998**, *110*, 1862; *Angew. Chem. Int. Ed.* **1998**, *37*, 1768d) R. J. Lee, L. Huang, *Crit. Rev. Ther. Drug Carrier Syst.* **1997**, *4*, 337; e) J.-P. Behr, *Bioconjugate Chem.* **1994**, *5*, 382.

[6] a) T. Merdan, J. Kopecek, T. Kissel, *Adv. Drug Delivery Rev.* **2002**, *54*, 715; b) S. J. Hwang, M. E. Davis, *Curr. Opin. Mol. Ther.* **2001**, *3*, 183; c) R. Kircheis, E. Wagner, *Gene Funct. Dis. Gene Ther. Reg.* **2000**, *1*, 95; d) S. C. De Smedt, J. Demeester, W. E. Hennink, *Pharm. Res.* **2000**, *17*, 113; e) M. C. L. Garnett, *Crit. Rev. Ther. Drug Carrier Syst.* **1999**, *16*, 147.

[7] a) A. V. Kabanov, V. A. Kabanov, *Bioconjugate Chem.* **1995**, *6*, 7; b) I. Jääskeläinen, J. Mönkkönen, A. Urtti, *Biochim. Biophys. Acta* **1994**, *1195*, 115.

[8] a) Y. Kakizawa, A. Harada, K. Kataoka, *Biomacromolecules* **2001**, *2*, 491; b) A. Harada, H. Togawa, K. Kataoka, *Eur. J. Pharm. Sci.*, **2001**, *13*, 35; c) S. V. Vinogradov, T. K. Bronich, A. V. Kabanov, *Bioconjugate Chem.* **1998**, *9*, 805; d) K. Kataoka, H. Togawa, A. Harada, K. Yasugi, T. Matsumoto, S. Katayose, *Macromolecules* **1996**, *29*, 8556; e) A. V. Kabanov, S. V. Vinogradov, Yu. Suzdaltseva, V. Yu. Alakhov, *Bioconjugate Chem.* **1995**, *6*, 639; f) A. Harada, K. Kataoka, *Macromolecules* **1995**, *28*, 5294.

[9] M. Oishi, S. Sasaki, Y. Nagasaki, K. Kataoka, *Biomacromolecules* **2003**, *4*, 1426.

[10] J. H. Jeong, S. W. Kim, T. G. Park, *Bioconjugate Chem.* **2003**, *14*, 473.

[11] J. Gruenberg, *Nat. Immunol. Nat. Rev. Mol. Cell. Biol.* **2001**, *2*, 721.

[12] a) C. H. Wu, G. Y. Wu, *Adv. Drug Delivery Rev.* **1998**, *29*, 243; b) M. Hashida, S. Takemura, M. Nishikawa, Y. Takakura, *J. Controlled Release* **1998**, *53*, 301; c) R. J. Stockert, *Physiol. Rev.* **1995**, *75*, 591.

[13] S. Cammas, Y. Nagasaki, K. Kataoka. *Bioconjugate Chem.* **1995**, *6*, 226.

[14] M. Mishra, J. R. Bennett, G. Chaudhuri, *Biochem. Pharmacol.* **2001**, *61*, 467.

[15] P. E. Stromhaug, T. O. Berg, T. Gjoen, P. O. Seglen, *Eur. J. Cell Biol.* **1997**, *73*, 28.

[16] M. A. Zanta, O. Boussif, A. Adib, J. P. Behr, *Bioconjugate Chem.* **1997**, *8*, 839.

[17] J. H. Jeong, S. W. Kim, T. G. Park, *J. Controlled Release* **2003**, *93*, 183.

[18] S. L. Goh, N. Murthy, M. Xu, J. M. J. Fréchet, *Bioconjugate Chem.* **2004**, *15*, 467.

[19] H. M. Moulton, M. H. Nelson, S. A. Hatlevig, M. T. Reddy, P. L. Iversen, *Bioconjugate Chem.* **2004**, *15*, 290.

[20] O. Boussif, F. Lezoualc, M. A. Zanta, M. D. Mergny, D. Scherman, B. Demeneix, J. P. Behr, *Proc. Natl. Acad. Sci. USA* **1995**, *92*, 7297.

[21] N. D. Sonawane, F. C. Szoka, A. S. Verkman, *J. Biol. Chem.* **2003**, *278*, 44826.

Received: September 16, 2004
Published online on March 8, 2005

J|A|C|S
COMMUNICATIONS

Published on Web 02/11/2005

PEGylated Polyplex Micelles from Triblock Catiomers with Spatially Ordered Layering of Condensed pDNA and Buffering Units for Enhanced Intracellular Gene Delivery

Shigeto Fukushima,[†,§] Kanjiro Miyata,[†,#] Nobuhiro Nishiyama,[*,‡] Naoki Kanayama,[†,#] Yuichi Yamasaki,[†,#] and Kazunori Kataoka[*,†,‡,#]

Department of Materials Science and Engineering, Graduate School of Engineering, The University of Tokyo, 7-3-1 Hongo, Bunkyo-ku, Tokyo 113-8656, Japan, Center for Disease Biology and Integrative Medicine, Graduate School of Medicine, The University of Tokyo, Tokyo 113-0033, Japan, Nippon Kayaku Co., Ltd., and CREST, Japan Science and Technology Agency, Japan

Received September 29, 2004; E-mail: nishiyama@bmw.t.u-tokyo.ac.jp; kataoka@bmw.t.u-tokyo.ac.jp

Successful in vivo gene therapy relies on the development of efficient gene vectors. Especially, the synthetic vectors based on cationic polymers have been attracting much attention because of their safety for clinical application and the variety of their chemical design. Nevertheless, the rational design of synthetic vectors remains to be established. Many previous studies have described that polyplexes formed from polycations with a comparatively low pK_a values, such as polyethylenimine (PEI), show a high transfection activity,[1] which has been explained by the proton sponge effect.[2] However, such polycations have a weak affinity to DNA, resulting in the formation of polyplexes that are easily dissociated under physiological conditions. Also, the buffer capacity of polycations may be hampered by their facilitated protonation due to the zipper effect or the neighboring group effect during the complexation process with DNA.[3] These problems could be modulated by the addition of excess polycations (i.e., increasing the N/P ratios[4]) to form polyplexes with a cationically deviated composition. However, it was recently demonstrated that free polycations in such polyplexes substantially contribute to efficient transfection but also mediate toxic effects. Hence, polyplex systems useful for in vivo gene delivery are required to achieve efficient transfection under the condition without free polycations.[5] Also, the gene delivery systems need to be equipped with high stability and biocompatibility. Here, A−B−C type triblock copolymers consisting of three distinctive functional segments were newly designed for constructing gene delivery systems which might not require free polycations to achieve enhanced gene expression but might provide a high stability and biocompatibility. In the present design of triblock copolymers, poly(ethylene glycol) (PEG) was used as the biocompatible A-segment, poly[(3-morpholinopropyl) aspartamide] (PMPA) was used as the low-pK_a B-segment with a buffering capacity, and poly(L-lysine) (PLL) was used as the high-pK_a C-segment to condense the DNA (Figure 1).

The triblock copolymer, PEG−PMPA−PLL, was synthesized by the successive ring-opening polymerization of the *N*-carboxyanhydrides (NCAs) of β-benzyl-L-aspartate (BLA) and ϵ-(benzyloxycarbonyl)-L-lysine (Lys(Z)), initiated by the $-NH_2$ group of α-methoxy-ω-amino PEG (MW 12 000), followed by the aminolysis of the benzyl ester of PBLA using 4-(3-aminopropyl)morpholine and the deprotection of the Z groups of PLL(Z).[6] The triblock copolymer was confirmed to have a narrow molecular weight distribution (M_w/M_n = 1.18), and the number of repeating units of PMPA and PLL was calculated to be 36 and 50, respectively, from the ^{1}H NMR. Diblock copolymers, PEG−PLL with 48 PLL units and PEG−PMPA with 39 PMPA units, were used as comparative samples in this study. The formation of polyplex micelles from these block catiomers was confirmed by a gel retardation assay (Figure S4, Supporting Information).[6] Also, the interaction between the di- or triblock copolymers and plasmid DNA (pDNA) was evaluated by an ethidium bromide (EtBr) exclusion assay (Figure 2a). In the case of PEG−PLL (pK_a 9.4), the fluorescence intensity was decreased to 20% of that of the naked pDNA at the N/P ratio of 2. In contrast, the system of PEG−PMPA, having a cationic segment with a lower pK_a value (pK_a 6.2), maintained relatively high fluorescence (>90%) over a wide range of N/P ratios, suggesting that PEG−PMPA lacks the capacity to condense pDNA to a level detectable by this assay. On the other hand, PEG−PMPA−PLL exhibited an 80% decrease in fluorescence at the N/P ratio of 3. Interestingly, the fluorescence profile of PEG−PMPA−

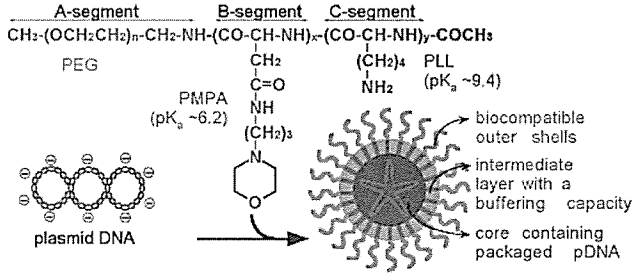

Figure 1. Chemical structure of PEG−PMPA−PLL triblock copolymers and schematic illustration of the hypothesized three-layered polyplex micelles with spatially regulated structure.

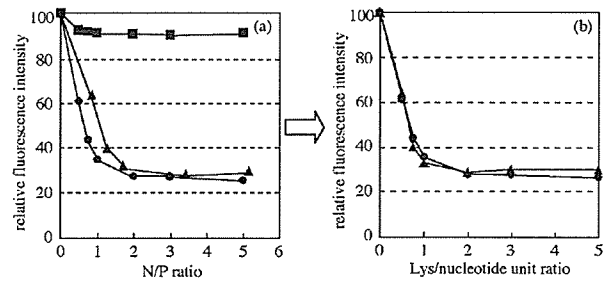

Figure 2. Interaction of PEG−PLL (circle), PEG−PMPA (square), and PEG−PMPA−PLL (triangle) copolymers with pDNA in 10 mM PBS (pH 7.4) + 150 mM NaCl, evaluated by dye exclusion assay. (a) In this figure, the *X*-axis represents the N/P ratio, where N stands for the total of MPA and Lys units. (b) In this figure, the *X* axis represents the Lys/nucleotide unit ratio.

† Graduate School of Engineering, The University of Tokyo.
‡ Graduate School of Medicine, The University of Tokyo.
§ Nippon Kayaku Co., Ltd.
# CREST, Japan Science and Technology Agency.

10.1021/ja0440506 CCC: $30.25

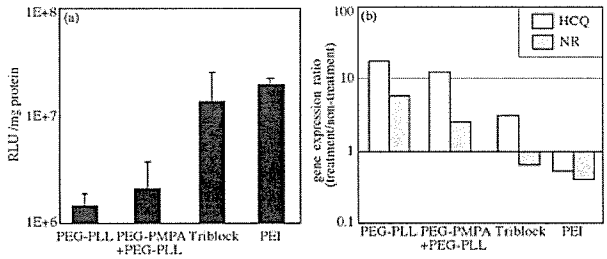

Figure 3. In vitro transfection of luciferase gene to HeLa cells by polyplex micelles from di- or triblock copolymers. HeLa cells were incubated with each micelle in the medium containing 10% serum for 24 h, followed by an additional 24 h incubation without the micelles. (a) The polyplex micelles were prepared at a Lys/nucleotide ratio of 2, and the PEI/pDNA was prepared at the corresponding N/P ratio to the PEG−PMPA−PLL/pDNA. (b) The effects of HCQ and NR on the TE of the polyplexes were evaluated. The PEI polyplex was prepared at the N/P ratio of 10.

PLL/pDNA was almost identical to that of PEG−PLL/pDNA when the N/P ratio was converted to the Lys/nucleotide unit ratio (Figure 2b). Presumably, in the complex of PEG−PMPA−PLL/pDNA, the PLL segment may predominantly contribute to the pDNA condensation. This assumption was confirmed by ^{1}H NMR measurement of PEG−PMPA−PLL/pDNA [Lys/nucleotide ratio = 2 (N/P ratio = 3.4)] in deutereted phosphate-buffered saline (pD 7.4, 150 mM NaCl), in which the chemical shifts assigned to the PLL segment completely disappeared but those assigned to the PMPA segments remained in the spectrum (Figure S6, Supporting Information).[6] This result is consistent with the hypothesis that the PEG−PMPA−PLL/pDNA may form three-layered polyplexes as illustrated in Figure 1. Also, the complete disappearance of PLL peaks from the NMR spectrum suggests that PEG−PMPA−PLL in free form may be minimal in the solution. The size and ζ-potential of the PEG−PMPA−PLL complexes at the Lys/nucleotide ratio of 2 were determined to be 88.7 nm and 7.3 mV, respectively, comparable to those obtained from the PEG−PLL complexes at the N/P ratio of 2 (91.7 nm and 2.1 mV, respectively). The particle size of approximately 100 nm is consistent with the condensed structure of pDNA, and the low absolute value of the ζ-potential suggests the formation of the PEG palisade surrounding the polyplex core.

In vitro transfection efficiency (TE) of the PEG−PMPA−PLL/pDNA at the Lys/nucleotide ratio of 2 was evaluated against HeLa cells. Notably, PEG−PMPA−PLL/pDNA revealed 1 order of magnitude higher TE than PEG-PLL/pDNA (Figure 3a), which was comparable to that of the PEI/pDNA at the corresponding N/P ratio, without showing appreciable cytotoxicity (Figure S9, Supporting Information).[6] On the other hand, the TE of the system composed of (PEG−PMPA + PEG−PLL)/pDNA, where the contents and the repeating units of the PMPA and PLL segments were nearly equal to PEG−PMPA−PLL, was almost the same as that of PEG−PLL. Also, the polyplexes of PEG−PMPA showed no transfection activity over a wide range of N/P ratios (data not shown). These results strongly indicate the importance of aligning in tandem two types of polycations with different pK_a values in a single polymer strand. To study the mechanism of the transfection, the effects of hydroxychloroquine (HCQ) and nigericin (NR) on transfection behavior were investigated. HCQ is known to increase the TE of the polyplexes lacking a buffering capacity, whereas NR could decrease the TE of the polyplexes showing the proton sponge effect.[7] The PEG−PMPA−PLL/pDNA showed less effect of HCQ on enhancing the gene expression compared with the PEG−PLL/pDNA, while it showed an appreciable decrease in the TE in the presence of NR (Figure 3b). Similar trends were also confirmed for 293T cells (Figure S8, Supporting Information). These biological results are consistent with the hypothesis that the enhanced TE of the PEG−PMPA−PLL/pDNA may be attributed to the proton sponge effect. Thus, the buffering capacity of PMPA segment appears to be maintained in the PEG−PMPA−PLL/pDNA under the condition with low Lys/nucleotide ratio. The preferential contribution of the PLL segment to the DNA condensation may ensure the presence of the uncomplexed PMPA segment, even at a comparatively low N/P ratio, to work as a buffering unit.[6]

Nonviral gene vectors used in vivo must have a high stability to be tolerated under harsh conditions in the body. In our previous studies, polyplexes based on PEG−PLL showed a high serum tolerability[8] and prolonged blood circulation.[9] Although the PLL segments form stable polyplexes with pDNA, the transfection activity might be inefficient due to the lack of a proton buffering capacity. In contrast, polycations with a lower pK_a have a buffering capacity for the enhanced transfection but demand a high N/P ratio to achieve a high efficacy. Polyplexes formed at a high N/P ratio may not be useful for in vivo transfection ,due to stability and toxicity concerns.[5] The result reported here led to the novel design of nonviral gene vectors, overcoming the problems of conventional systems based on the proton sponge concept, using the A−B−C type triblock copolymers, PEG−PMPA−PLL (Figure 1). The results are consistent with the hypothesis that PEG−PMPA−PLL might form three-layered polyplex micelles consisting of a core of pDNA/PLL polyion complexes, an intermediate layer of PMPA segments with a buffer capacity, and an outer shell of biocompatible PEG segments. The PEG−PMPA−PLL polyplexes showed a significantly enhanced transfection activity through the buffering capacity of the PMPA segment, while efficiently compacting pDNA by the PLL segment. Importantly, this increased transfection was achieved under the condition where free or loosely associated polycations are assumed to be minimal, facilitating the future utility of this polyplex micelle for in vivo gene delivery.

Acknowledgment. This work was supported by the Core Research for Evolutional Science and Technology (CREST) from the Japan Science and Technology Agency (JST).

Supporting Information Available: Synthetic method and characterization of triblock copolymers as well as additional data on the physicochemical and biological properties of the PEG−PMPA−PLL/pDNA. This material is available free of charge via the Internet at http://pubs.acs.org.

References

(1) (a) Boussif, O.; Lezoualc'h, F.; Zanta, M. A.; Mergny, M. D.; Scherman, D.; Demeneix, B.; Behr, J.-P. *Proc. Natl. Acad. U.S.A.* **1995**, *92*, 7297−7301. (b) Tang, M. X.; Szoka, F. C. *Gene Ther.* **1997**, *4*, 823−832. (c) Midoux, P.; Monsigny, M. *Bioconjugate Chem.* **1999**, *10*, 406−411. (d) Cherng, J.-Y.; Wetering, P.; Talsma, H.; Crommelin, D. J. A.; Hennink, W. E. *Pharm. Res.* **1996**, *13*, 1038−1042.
(2) Behr, J.-P. *Chemia* **1997**, *51*, 34−36.
(3) Kabanov, A. V.; Bronich, T. K.; Kabanov, V. A.; Yu, K.; Eisenberg, A. *Macromolecules* **1996**, *29*, 6797−6802.
(4) The ratio of the cationic moiety in polycations to the phosphate in DNA.
(5) Boeckle, S.; Gersdorff, K.; Piepen, S.; Culmsee, C.; Wagner, E.; Ogris, M. *J. Gene Med.* **2004**, *6*, 1102−1111.
(6) See Supporting Information.
(7) Lim, Y.-B.; Kim, S.-M.; Suh, H.; Park, J.-S. *Bioconjugate Chem.* **2002**, *13*, 952−957.
(8) (a) Itaka, K.; Harada, A.; Nakamura, K.; Kawaguchi, H.; Kataoka, K. *Biomacromolecules* **2002**, *3*, 841−845. (b) Itaka, K.; Yamauchi, K.; Harada, A.; Nakamura, K.; Kawaguchi, H.; Kataoka, K. *Biomaterials* **2003**, *24*, 4495−4506.
(9) Harada-Shiba, M.; Yamauchi, K.; Harada, A.; Takamisawa, I.; Shimokado, K.; Kataoka, K. *Gene Ther.* **2002**, *9*, 407−414.

JA0440506